INFORMATION TO USERS

This manuscript has been reproduced from the microfilm master. UMI films the text directly from the original or copy submitted. Thus, some thesis and dissertation copies are in typewriter face, while others may be from any type of computer printer.

The quality of this reproduction is dependent upon the quality of the copy submitted. Broken or indistinct print, colored or poor quality illustrations and photographs, print bleedthrough, substandard margins, and improper alignment can adversely affect reproduction.

In the unlikely event that the author did not send UMI a complete manuscript and there are missing pages, these will be noted. Also, if unauthorized copyright material had to be removed, a note will indicate the deletion.

Oversize materials (e.g., maps, drawings, charts) are reproduced by sectioning the original, beginning at the upper left-hand corner and continuing from left to right in equal sections with small overlaps.

ProQuest Information and Learning
300 North Zeeb Road, Ann Arbor, MI 48106-1346 USA
800-521-0600

FOAM SEPARATION OF

ETHYLHEXADECYLDIMETHYLAMMONIUM BROMIDE

by

TRAN TRACH

A thesis submitted in partial fulfillment

of the requirements for the degree of

MASTER OF SCIENCE

in the

DEPARTMENT OF CHEMICAL ENGINEERING

UNIVERSITY OF OTTAWA

Ottawa, Canada

January, 1966

Approved by

M. Sc. Candidate

ACKNOWLEDGMENT

The author wishes to acknowledge his sincere gratitude to Dr. B. C.-Y. Lu for providing the facilities for this research work, to Dr. R. K. Wood, who directed its course, for his advice and encouragement, to Mr. G. Gasperetti for his technical assistance, and to Mrs. L. Carriere for typing the manuscript.

Finally, the author wishes to express his sincere thanks to the National Research Council, Ottawa, for providing the financial assistance through Research Grant No. A-1944.

ABSTRACT

The adsorption of ethylhexadecyldimethylammonium bromide (EHDA-Br) at liquid-air interfaces generated by bubbling a constant stream of air through an aqueous solution was determined with a 2 in. diameter foam separation column equipped with a gas sparger made of porous stainless steel (20 μ pores). The results obtained from batch operation with total recirculation of the collapsed foam as well as from continuous operation showed that the surface excess Γ depends on foam rate as well as bulk concentration whereas Gibbs' adsorption isotherm predicts a constant value for Γ. It was concluded that the application of Gibbs' equation to the prediction of the surface excess accumulated at dynamic interfaces generated in the foam separation process for EHDA-Br is probably justified only under the rather stringent conditions of good drainage and perfect stability of the foam. Equations proposed to predict the performance characteristics of a continuous pool-feed foam separation column based on Gibbs' equation and an ideal foam model were also found to be valid under the same conditions.

The effect on the various parameters describing the efficiency of a continuous foam separation column was studied for the following

variables: feed concentration, foam column height, feed rate, column diameter.

An attempt was also made to analyze the continuous foam separation process by utilizing the concept of the HTU.

TABLE OF CONTENTS

LIST OF TABLES

LIST OF FIGURES

I INTRODUCTION

Foam separation is a new separation technique which takes advantage of the fact that certain solutes, due to their surface activity, collect at a liquid-gas interface generated by bubbling an inert gas through a solution. The increased attention which foam separation is now receiving is due to the fact that, unlike the conventional methods available for the separation of homogeneous liquid mixtures, its efficiency improves with decreasing concentration.

The recovery of substances of high unit value but found in low concentration during metallurgical processes, the treatment of secondary sewage effluents containing non-biodegradable detergents, the decontamination of radioactive wastes, require a method of separation with high efficiency at low concentrations, which is characteristic of foam separation.

Despite the potentialities of this separation technique, quantitative data published are still scarce and no general process design method exists.

The objective of this work is:

(1) to measure the adsorption of a surfactant at the liquid-gas interface generated by bubbling a constant stream of air through a surfactant-water solution.

(2) to assess the applicability of Gibbs' adsorption isotherm to non-static interfaces encountered in the foam separation process.

(3) to study the effect of various operating variables on the performance of a continuous foam separation column.

(4) to analyze the process from a chemical engineering point of view.

The system investigated is water-ethylhexadecyldimethyl-ammonium bromide (EHDA-Br), a cationic surfactant. The choice of this surfactant was prompted by the fact that most of published data are concerned with anionic surfactants and by consideration of possible use for further work in ion flotation.

II LITERATURE SURVEY

1. Foam Separation in Chemistry and Biology

Foam separation has always interested chemists and biologists who found the technique particularly suitable for the concentration and purification of enzymes, proteins and similar biological materials. In 1936, Ostwald and Siehr (1) separated sodium oleates and aluminum stearates and concentrated albumin from urine by foaming with carbon dioxide. Ostwald and Mischke (2) separated "patent blue" and "new coccine" from an aqueous solution of these two dyes. Dubrisay (3) separated the riccinic acids from fatty acids. More recently Schnepf and Gaden (4) investigated the effect of pH and concentration upon the separation obtaining by foaming aqueous solutions of bovine serum albumin and glucose polymer dextran. They found that optimum separation occurs at the isoelectric pH. London et al (5) also found an optimum point close to the isoelectric point for the separation of jackbean urease (an enzyme). An exhaustive list of studies performed on dyes, proteins, enzymes and other miscellaneous substances up to 1961 is reported in the excellent review by Rubin and Gaden (6). The interest of biologists and chemists in foam separation arises from the fact that it is very often the only method suitable for substances exhibiting an extreme sensitivity to heat, pH, solvents, etc. For instance, Boyles and Lincoln (7) used this technique to remove and concentrate bacterial spores and vegetative cells from culture medium.

These applications, however, are not very interesting from an engineering point of view since they were realized only on a small scale, and almost always conducted as batch processes.

2. Continuous Foam Separation

Continuous foam separation has been recently investigated for two main types of applications:

(a)- treatment of waste water contaminated with soluble surface-active organic materials which resist conventional purification methods.

(b)- removal of ions made surface-active by complexing them with a collector (ion flotation).

a. Waste Water Treatment: Surfactant Removal

Water quality is seriously affected by contamination with soluble organic materials including detergents, insecticides, phenolic compounds, benzene derivatives, and simple hydrocarbon derivatives. This pollution is caused by both domestic and industrial wastes. Most soluble organic compounds are surface-active and can therefore be naturally concentrated by foaming.

Eldib (8) first suggested foam separation for the removal of soluble organic water contaminants ranging from synthetic detergents to natural materials derived from the life cycle of aquatic plants. Kevorkian and Gaden (9) conducted exploratory studies on the foaming of isobutyl

alcohol. Rubin and Everett (10) have reported data concerning the removal of alkylbenzene sulfonate (ABS), an anionic surfactant frequently encountered in synthetic detergents. Lemlich et al (11, 12) investigated the effects of various operating variables, including reflux ratio, on the separation of Aresket-300 and Triton X-100. Extensive quantitative and qualitative results have been reported for sodium dodecylsulfate (SDS) by Kishimoto (13). Grieves et al (14) conducted experiments on ABS and SDS. Grieves and Wood (15) have proposed a continuous process for the treatment of refining and petrochemical wastes.

b. Ion Flotation

Ion flotation is the process of removing ions from a solution by complexing them with a surface active agent followed by foaming. The resulting complex, or chelate must, of course, be surface active and capable of producing a reasonably stable foam. The development of this technique is quite recent but it has already shown tremendous potential, especially for the decontamination of radioactive wastes. Studies on uranyl ions (UO_2^{++}), has been performed by Rubin (16). Data concerning the removal of other products of fission (Cs^{+}, Sr^{++}, Ce^{+++}) from radioactive effluent streams, have been reported by Schonfeld et al (17, 18, 19) and also by Banfield et al (20). It should be noted that all

of these studies have been conducted with anionic surfactants. An extensive discussion of ion flotation, and a complete study, group by group, of metals that can be separated by ion flotation has been presented by Sebba (21).

3. Literature pertaining to EHDA-Br

The only cationic surfactant which has been subjected to extensive study in foam separation is EHDA-Br. Grieves and Wood have studied the effects of the following variables on the continuous foam separation of EHDA-Br:

- Foam-liquid solution interface, height of foam (22).
- Liquid residence time, position of feed introduction (23).

Grieves and Battacharyya have also reported the effects of temperature (24) and pH (25), and proposed correlations for the prediction of separation efficiency (26). Grieves and his coworkers (27, 28) have also reported results when using EHDA-Br as the complexing agent for the flotation of dichromate ion.

III THEORETICAL CONSIDERATIONS

1. The Nature of Foam

Foam is a coarse dispersion of a gas in a liquid. The liquid is the continuous phase although most of the volume is occupied by gas. The system differs from the other dispersions, in that it has a definite structure. The bubbles are arranged in such a manner that three films come together to form solid angles of 120° each. This configuration, which is shown in Figure 1, results from the interaction of surface tension and pressure difference and it has been established that this is the only stable configuration possible. The junction of three bubbles is of special importance. This was recognized by Plateau and this junction is called a Plateau border (29). The liquid in the Plateau border is at a lower pressure than the liquid in the film between the bubbles due to the smaller radii of curvature of the Plateau border. Hence, a pressure gradient exists from a plane wall to a junction, and the movement of liquid caused by this pressure gradient is responsible for foam drainage, in addition to the flow due to gravitation.

Due to drainage, foams can be divided into two extreme types. Wet foams, with a high liquid content, which consist of spherical bubbles, and dry foams whose bubbles are polyhedral in shape.

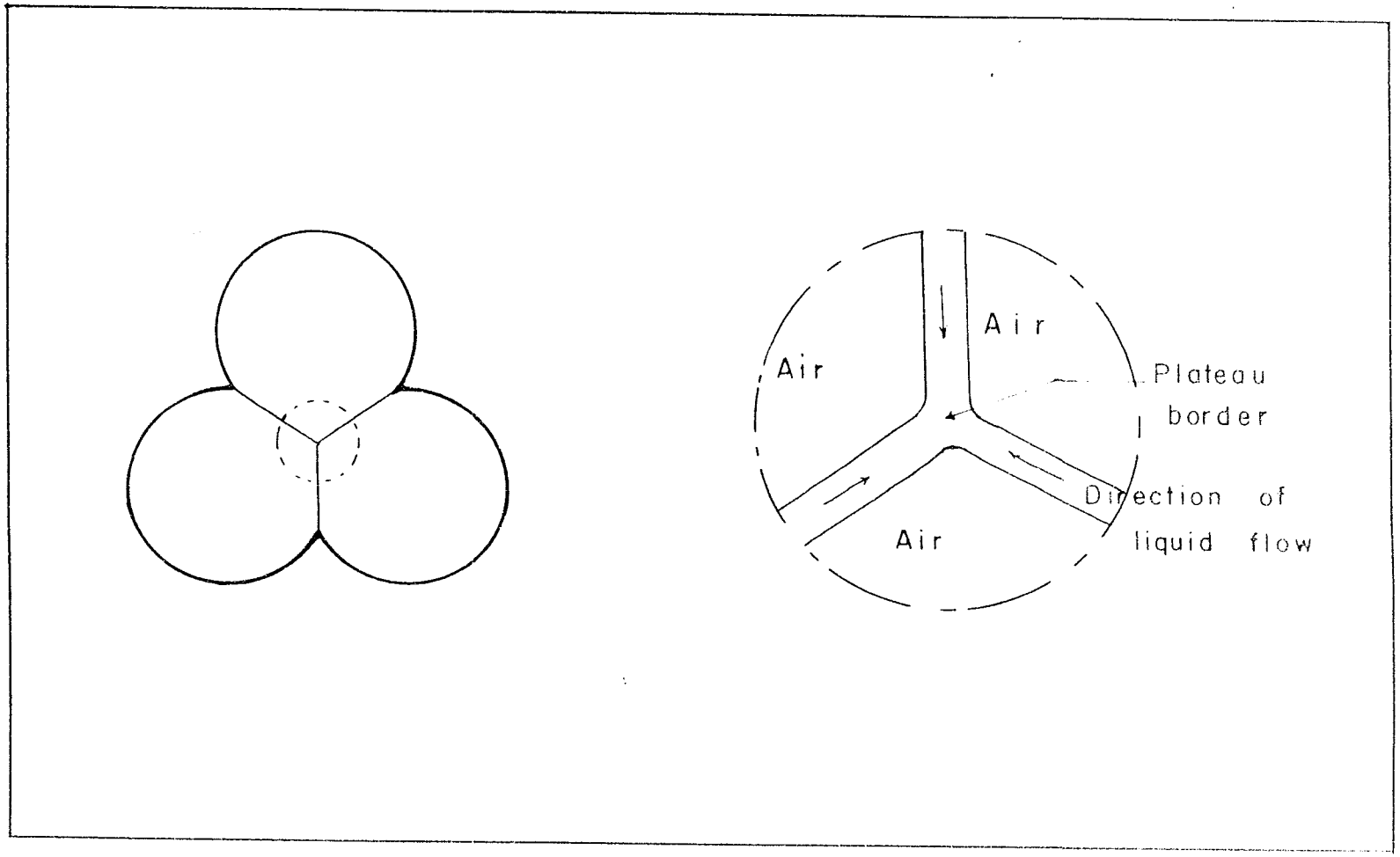

Figure 1. Stable Configuration of Bubbles and Plateau Border

Foams are formed by agitating the liquid and gas together in presence of a stabilizing agent or by blowing air through porous metals into the liquid. Sometimes foams are beneficial, but often they constitute a nuisance in some processes and in the operating of certain equipments, and therefore the foam must be prevented from forming or be destroyed. Beneficial uses of foams include fire-fighting, foamed plastics, foam separation.

2. Theories of Foam Formation

Plateau (33) first tried to relate foam formation with surface tension and stated that a liquid foams better the lower its surface tension. This, however, is not correct, because pure liquids do not foam at all, as shown experimentally by Foulk and Miller (34, 35). They established that both negatively and positively adsorbed dissolved matters cause foam in liquids and concluded that liquid films are formed by the mutual approach of two already formed surfaces. The two surfaces will not merge and subsequently vanish because of the resistance due to the difference in concentration between the surface layer and the bulk solution. Several other theories have been suggested to describe the formation of a foam. Hazlehurst and Neville (36) have proposed a "cybotactic" theory which is based on the premise that the liquid is composed of molecular swarms or "cybotactic" groups having only a transitory existence for lack of anchorage

or directive influence. This anchorage is provided by an interface of any type, where the cybotactic effects will be stronger and more persistent, possibly approaching the orderliness and stability of crystals. More recently, Nakagaki (37) advanced a thermodynamic theory of foam formation and foam stability, using as a basis foam volume and foam life.

3. Principles of Foam Separation and Ion Flotation

Foam separation, also known as foam fractionation, takes advantage of the distribution of the components of a solution between a bulk liquid phase and a mobile interfacial film between this phase and a gas phase. The interfacial film is generated by a constant gas stream. The distribution of the components of the solution between the bulk phase and the interfacial film is governed by a selective adsorption process. In order to be separated by foaming, a substance must lower the surface tension of the bulk liquid. This is the property of molecules which are soluble in water and which contain both a hydrophilic and a hydrophobic group. These substances are known as surface active agents or "surfactants". Their concentration at the surface of their aqueous solutions is due to a reorientation of the hydrophobic (organic) ends of the surfactant molecules towards the gas-solution interface in order to minimize contact

with the solution. As a result, a surface layer is formed which contains an excess of surfactant over that contained in the bulk solution. The driving force which causes the migration of these molecules to the interface is considered to be the excess surface-free energy of the molecule in the bulk solution over that associated with the molecule when it is in the surface layer.

Non-surface-active materials, such as metallic ions, cannot naturally be concentrated by foaming. A surface-active ion, of opposite charge to the ion that is to be concentrated, must be added to the solution. Gas bubbles are then introduced into the solution, a foam is formed which collects the surface-active material carrying with it the oppositely charged ion. This process is usually designated as being ion flotation. The phenomenon was first observed by Langmuir (31) who reported the sensitivity of monolayers to traces of metal ion impurities, especially copper and aluminum. The foam fractionation or ion flotation process should not be confused with froth flotation, a conventional method extensively used in ore dressing. Foam fractionation and froth flotation are mechanically similar in that both involve the gassing of a liquid mass. However, froth flotation deals with a heterogeneous system involving at least two, usually three different phases, a liquid and two different solids. Separation of the solids is achieved by modifying the particle surface characteristics of one by incorporating some "collecting agent", so that it is more readily attached

to air bubbles. Froth flotation is therefore a physical method employing an artificially magnified density difference, caused by a selective attachment of a solid to gas bubbles, between particles of different solids, and is analogous, in principle, to sedimentation. Foam separation, on the other hand, is used to separate the components of a single homogeneous liquid phase. The material which concentrates in the foam phase must have existed in true solution in the liquid medium. The distinction between foam fractionation and froth flotation, however, is not so clear in the case of the foam separation of colloid-surfactant systems, where the final effect is a combination of froth flotation resulting in the removal of colloid particulates and of foam separation resulting in an enrichment of the froth in surfactant (32).

4. Gibbs Adsorption Isotherm

The basis of the thermodynamics of the adsorption of dissolved substances at interfaces is Gibbs' Equation (38). It relates the degree of adsorption at the boundary between two phases in thermodynamic equilibrium and at a constant temperature to the change in interfacial tension at that boundary and the composition of the two phases:

$$d\gamma = -\Gamma_1 d\mu_1 - \Gamma_2 d\mu_2 - \ldots\ldots \Gamma_i d\mu_i \ldots\ldots - \Gamma_n d\mu_n \quad (1)$$

where γ = interfacial or surface tension

Γ = surface excess of the components (1, 2, ... i, ..., n)

μ = chemical potential of the components (1, 2, i, n).

Equation (1) is the strict Gibbs equation for adsorption and is rigorously as correct as are the Laws of Thermodynamics from which it is derived. The summation on the right hand side of eq. (1) must, however, include all adsorbed species, including the counter-ions if the solute consists of long-chain ions (39).

With the introduction of activity and its definition

$$\mu_i = \mu_i^{\circ} + RT \ln a_i \qquad (2)$$

where μ_i° = standard chemical potential of species i

R = gas constant

Equation (1) becomes

$$d\gamma = - RT \sum \Gamma_i \, d \ln a_i \qquad (3)$$

The numerical value of the surface excess depends on its definition. In order to assign numerical values to the Γ terms, it is necessary to define a mathematical interface at some arbitrary position at or near the interface. The validity of equation (1) is not affected by the position chosen for this mathematical interface provided it is planar.

Defining the mathematical plane so that the surface excess of the solvent is zero according to the convention of Gibbs (38) or of Guggenheim and Adam, the summation of equation (3) involves only terms for the solute.

a. Gibbs' Equation for Very Dilute Solutions

For ideal solutions, concentration can be used instead of activity, and eq. (3) reduces to

$$d\gamma = -RT\sum\Gamma_i \, d \ln x_i \qquad (4)$$

This simplified form of Gibbs' equation is often used since solutions under consideration are generally dilute and nearly ideal.

b. Adsorption of EHDA-Br

Solutions of anionic or cationic surface-active agents may be considered as electrolyte solutions. According to Brady and Brown (41), Cockbain and McMullen (42), the uni-univalent surfactant is considered to be completely dissociated. Thus, in the interfacial layer of the system EHDA-Br-Water the following species: EHDA-Br and EHDA-OH will be present as a result of the hydrolysis of the quaternary ammonium salt. Consequently, there exists the possibility of the adsorption of the following ions in the monolayer:

$$EHDA^+, \; Br^-, \; OH^-$$

Therefore

$$-d\gamma = RT\,\Gamma_{EHDA^+} \, d \ln x_{EHDA^+} + RT\,\Gamma_{Br^-} \, d \ln x_{Br^-} + RT\,\Gamma_{OH^-} \, d \ln x_{OH^-}$$

Since quaternary ammonium salts do not hydrolyse appreciably in dilute solutions (25) the pH of the bulk solution does not change markedly with changes in concentration. Hence $d \ln x_{OH^-} = 0$ and this term can be

neglected. Furthermore $x_{Br^-} = x_{EHDA^+} = x_{EHDA\ Br}$ for complete dissociation of the electrolyte and if there is no adsorption of OH^- in the interface, which is the assumption usually employed, then

$$\Gamma_{OH^-} = 0, \quad \Gamma_{Br^-} = \Gamma_{EHDA^+} = \Gamma_{EHDA\text{-}Br}$$

and it follows that

$$\Gamma_{EHDA^+} = \Gamma_{EHDA\text{-}Br} = \frac{-1}{2\,RT} \frac{d\gamma}{d \ln x_{EHDA\text{-}Br}} \qquad (5)$$

If OH^- is adsorbed rather than Br^-, then $\Gamma_{Br^-} = 0$, $\Gamma_{EHDA^+} = \Gamma_{EHDA\text{-}OH}$

$$\Gamma_{EHDA^+} = \Gamma_{EHDA\text{-}OH} = \frac{-1}{RT} \frac{d\gamma}{d \ln x_{EHDA\text{-}Br}} \qquad (6)$$

Thus with surface hydrolysis and preferential adsorption of OH^- (or H^+ in the case of an anionic surfactant), the numerical value of Γ is double that calculated on the basis of no hydrolysis.

The application of Gibbs' equation has given rise to some confusion, mostly because all adsorbed species are not considered. Many cases are reported in the literature (43, 44) where surface hydrolysis or preferential adsorption of undissociated molecules are not assumed and yet equation (6) is used, whereas equation (5) would be the correct form. An extensive discussion of Gibbs' equation is given in the book by Davies and Rideal (39).

Instead of using concentrations in lieu of activities, a more rigorous form of Gibbs' equation can be obtained using the Debye-Huckel expression for the activity coefficient. Below the critical micelle concentration, colloidal electrolytes behave as ordinary uni-univalent electrolytes, and the following equation has been applied (41):

$$\frac{d \ln a_i}{d \ln x_i} = 2 (1 - 0.6 \sqrt{x_i}) \qquad (7)$$

A more rigorous form of eq. (5) would then be

$$\Gamma_{EHDA^+} = \Gamma_{EHDA\text{-}Br} = \frac{-1}{2 RT (1 - 0.6 \sqrt{x}_{EHDA\text{-}Br})} \frac{d\gamma}{d \ln x_{EHDA\text{-}Br}} \qquad (8)$$

However, the correction factor $0.6 \sqrt{x}$ is negligible for dilute solutions encountered in this work and the use of equation (5) is justified.

c. Other Adsorption Equations

For certain special cases of adsorption, there exist more specific adsorption isotherms. Langmuir's equation (45) is valid for very dilute solutions of un-ionized solutes but unapplicable for the adsorption of ions, as is Szyskowski's empirical relationship (39). For the derivation and interpretation of the various adsorption isotherms that have been proposed the reader is referred to surface chemistry books (29, 30, 39).

5. The Ideal Foam Model

In an attempt to understand the foam separation process, an ideal foam model has been used by several authors (6, 20, 26). This

model involves a number of significant simplifications which must not be overlooked but which prove quite reasonable under specific conditions.

a. Basic Concepts of the Ideal Foam Model

The ideal foam model is based on the following assumptions:

(1) The foam is composed of spherical bubbles. Generally, the size of the bubbles is not uniform, and an effective average diameter based on volume and surface must be used.

$$D_{eff} = \frac{\sum D^3}{\sum D^2} \tag{9}$$

(2) There is no bubble breakage in the foam before exit from the column. This implies complete foam stability and absence of internal reflux.

(3) Adsorption at the surface is instantaneous and the system is in equilibrium (in order to apply Gibbs' equation).

(4) The liquid mechanically entrained by the foam is of the same concentration as the bulk liquid. Employing these assumptions, the following expression can be stated:

$$y_s = x_B + \Gamma A \tag{10}$$

where y_s = concentration of the surfactant in the surface layer at equilibrium (g/cm^3)

x_B = concentration of the surfactant in the bulk solution (g/cm^3)

Γ = surfactant surface excess (g/cm^2)

A = interfacial area per unit volume of surface layer (cm^2/cm^3)

The number of bubbles per unit volume of foam is $6/(\pi D^3)$ since the volume occupied by the liquid is negligible.

Interfacial area per unit volume of foam: $6\pi D^2/\pi D^3 = 6/D$ (11)

Interfacial area per unit volume of surface layer:

$$A = \frac{6}{D}\ \frac{G}{S} \tag{12}$$

where

G = volumetric foam rate (cm^3/min)

S = volumetric surface layer rate (cm^3/min)

b. Single-Stage Equilibrium Column

An equilibrium relationship between the concentration of the solute in the foam liquid (also called foamate by analogy with the distillate), and its concentration in the bulk liquid can be obtained by conducting a batch separation operation with total recirculation of foamate in order to keep the bulk concentration constant.

For the system represented in Fig. 2, the material balance on the surfactant is:

$$Fy_F = Fx_B + SA\Gamma \tag{13}$$

where F = volumetric foamate rate (cm^3/min)

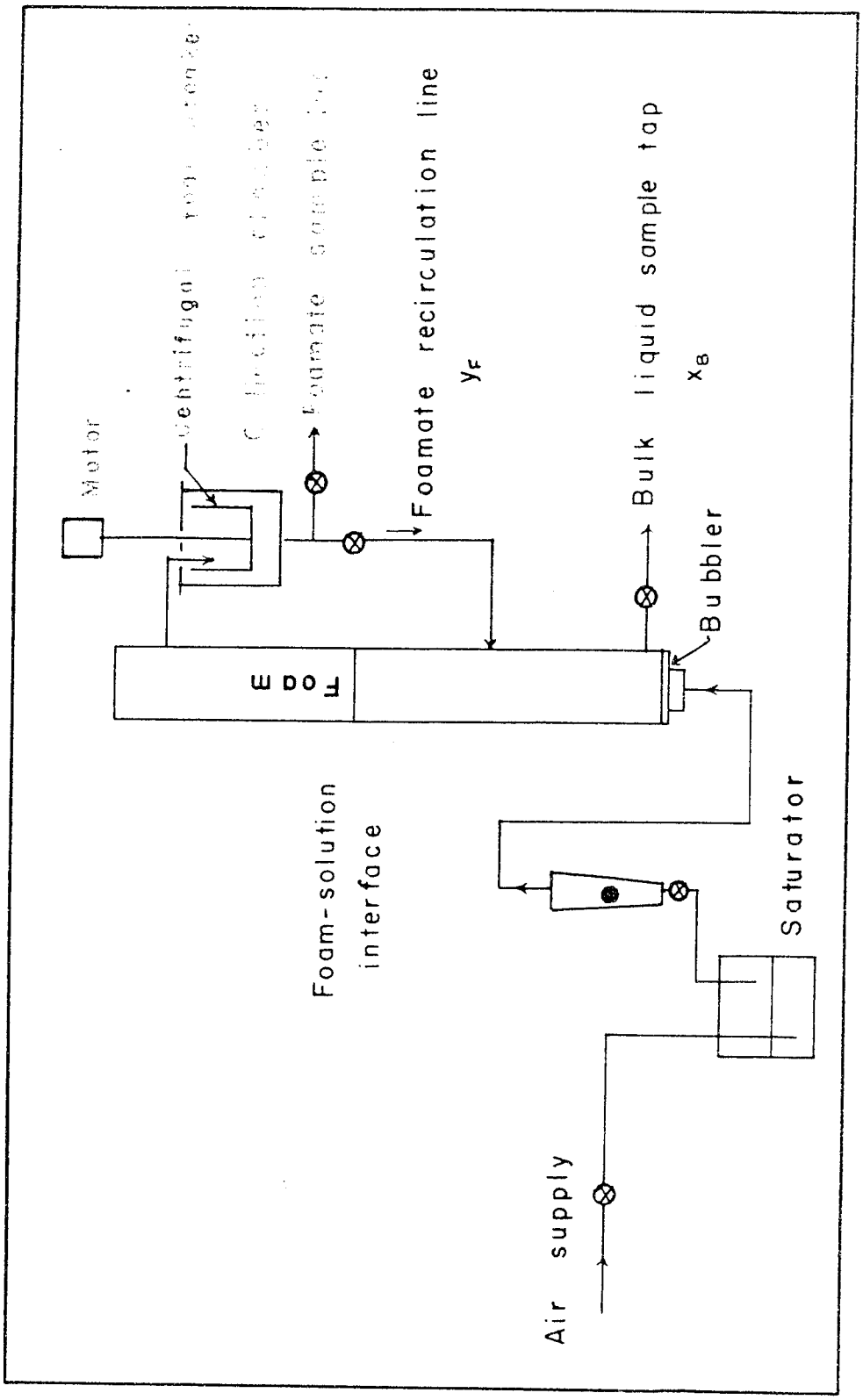

Figure 2. Schematic Flow Diagram of Apparatus for Total Reflux Operation

Combining this equation with eq. (12) yields

$$\Gamma = (y_F - x_B) \frac{DF}{6G} \tag{14}$$

or:

$$\Gamma = (E - 1) \frac{D\,l\,x_B}{6} \tag{15}$$

where $E = y_F/x_B$ = Enrichment ratio

$$l = \frac{F}{G} = \frac{\text{ml liquid}}{\text{ml foam}} = \text{Foam ratio}$$

Equation (15) will be used to calculate Gibbs' adsorption from total reflux data.

c. Continuous Foam Separation

For the continuous foam separation column, where the feed of concentration x_L is introduced continuously below the solution-foam interface at a rate L and collapsed foam of concentration y_F and bulk solution of concentration x_B are withdrawn continuously at the top and the bottom of the column at rates F and B respectively (Fig. 3), the following material balance equations can be written at steady-state:

$$L = F + B \tag{16}$$

$$Fy_F = Fx_B + SA\Gamma \tag{17}$$

$$Lx_L = Fy_F + Bx_B \tag{18}$$

or

$$Fy_F = Sy_S + (F - S)\,x_B \tag{19}$$

The second term of the right hand side of equation (19) represents the contribution of the liquid entrained by the rising foam which is assumed to be of the same concentration as the liquid pool.

The following conditions are implied in equations (17 - 19).

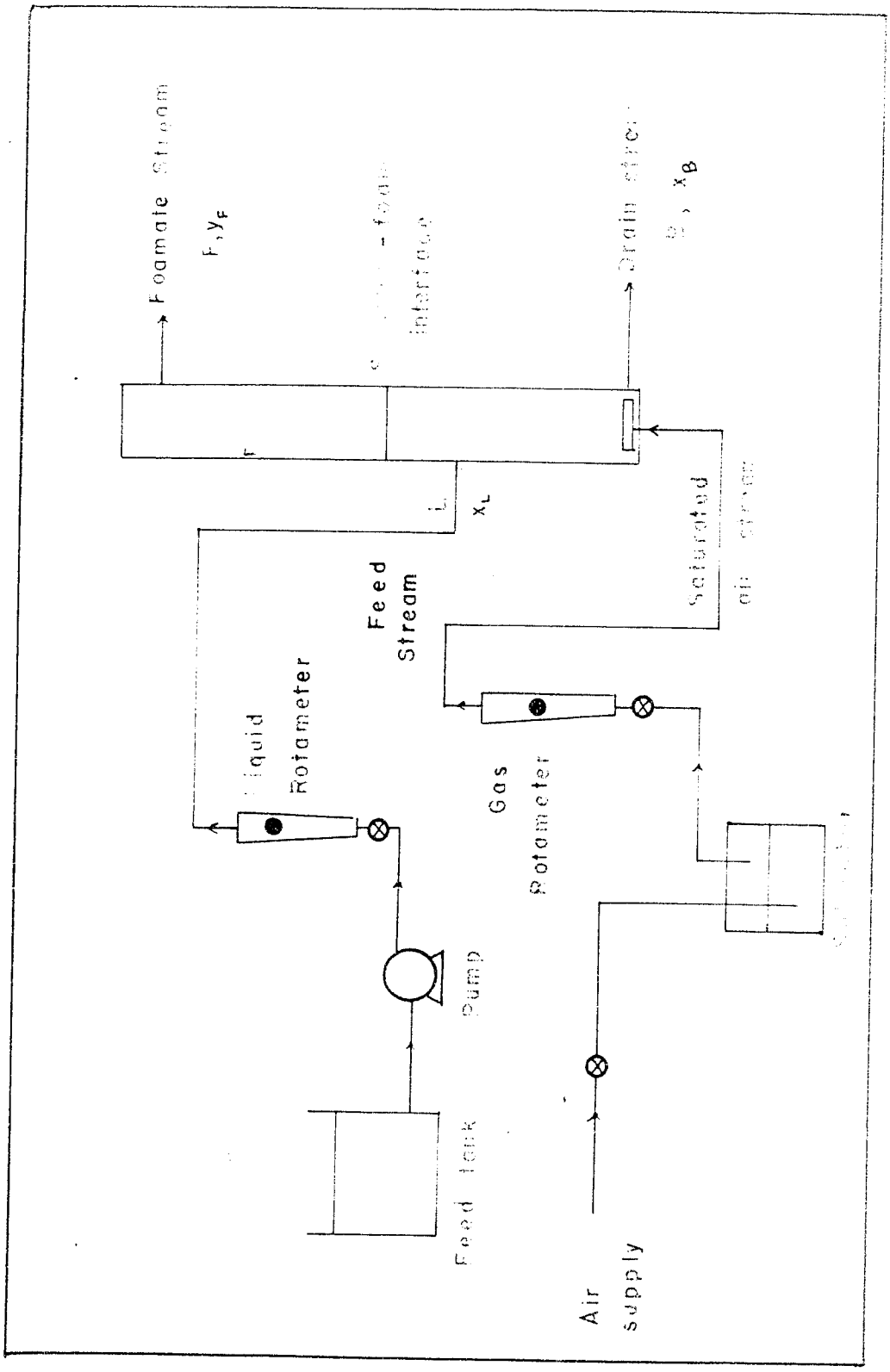

Figure 3. Schematic Flow Diagram of Apparatus for Continuous Operation

(1) - The liquid pool is well mixed, without concentration gradient, i.e. the bottom concentration is the same as that in the liquid pool.

(2) - The column operates as a single equilibrium stage, i.e. there is no enrichment due to internal reflux brought about by bubble breakage in the foam column.

From equations (16 - 19) and Gibbs' adsorption isotherm (eq. (5)), the following relations can be derived:

$$y_F - x_B = -\frac{3}{RTD}\frac{d\gamma}{d \ln x_B}\frac{G}{F} \tag{20}$$

$$x_L - x_B = -\frac{3}{RTD}\frac{d\gamma}{d \ln x_B}\frac{G}{L} \tag{21}$$

$$y_F - x_L = -\frac{3}{RTD}\frac{d\gamma}{d \ln x_B}\frac{G}{F}\frac{B}{L} \tag{22}$$

Equations (20 - 22) can theoretically be used to predict the overhead and bottoms concentrations for given feed concentration, feed rate and foam rate provided the following information is available:

(1) - Relationships between B, F, D at given feed concentration, feed rate and gas rate

(2) - Surface tension - concentration data

Very often, as in the case of EHDA-Br, $d\gamma/d \ln x_B$ is constant for a wide concentration range below the critical micelle concentration. If such is the case, a plot of

$(y_F - x_B)\,DF$, $(x_L - x_B)\,DL$ and $(y_F - x_L)\,\frac{DFL}{B}$ versus G should result in a straight line with slope $\frac{-3}{RT}\,\frac{d\gamma}{d \ln x_B}$.

Furthermore, since $(y_F - x_B)\,DF$, $(x_L - x_B)\,DL$ and $(y_F - x_L)\,DFL/B$ are all equal to $\frac{-3}{RT}\,\frac{d\gamma}{d \ln x_B}\,G$, their values must be equal for a given foam rate.

Rearranging and combining equations (16 - 19) shows that the surface excess can be evaluated from

$$\Gamma_B = \left(\frac{x_L}{x_B} - 1\right)\left(\frac{L}{G}\,\frac{D}{6}\right) x_B \qquad (23)$$

or:

$$\Gamma_F = \left(\frac{y_F}{x_B} - 1\right)\left(\frac{F}{G}\,\frac{D}{6}\right) x_B \qquad (24)$$

These two equations are equivalent since they result from the same set of equations, and the numerical values of Γ_B and Γ_F should be equal if the data are consistent.

IV APPARATUS AND EXPERIMENTAL PROCEDURE

1. Apparatus

a. Outline of the Experimental Apparatus

Figures 2 and 3 represent the experimental apparatus for total reflux and continuous operations respectively. In both cases, air which is obtained from a compressed air cylinder passes through a pressure regulator which reduces the line pressure to approximately 3 psig. It is then saturated with water to prevent evaporation in the foam column, and its flow rate adjusted by a valve and measured by a gas rotameter before it passes to the gas sparger.

For the single-stage equilibrium studies, a series of tests were conducted with no feed make-up and at total reflux, that is, the foam at the top of the column is collapsed and completely recirculated.

In continuous operation, the feed, which was stored in a polyethylene reservoir, was pumped into the column at a constant rate as measured by a rotameter and a foam and a drain stream were withdrawn at the top and the bottom of the column respectively.

b. Foam Columns

Three columns, with diameters of 2, 4 and 6 inches, (all 6 feet in height) made of Lucite plastic were used in this study. The 4 in.

column, had 3/4 in. holes, spaced 4 in. apart to provide alternate feeding and foam removal locations.

c. Bubblers

The bubblers were made from porous steel metal purchased from:

Pall Trinity Micro Corporation

Cortland, New York, U.S.A.

Metal specifications: grade F, mean pore size: 20 microns, nominal thickness: 1/8 in. For use with the 4 in. and 6 in. column a porous metal plate of 2.5 in. in diameter was cut from the porous metal sheet and a short section of 2.5 in. diameter stainless steel tube was soft soldered to the porous metal plate. For the 2 in. column, a 2 in. plate was attached directly to the bottom of the column.

d. Saturator

Before being admitted into the bubbler, the air stream was passed through a fritted glass tube contained in a bottle filled with distilled water. The air stream emerging from the saturator was humidified and thus prevented water from evaporating from the EHDA-Br solution.

e. Foam breaker

For the equilibrium studies, it was essential that the bulk liquid was maintained at a constant concentration and to accomplish this,

the foam produced was collapsed and recirculated in its entirety. It was found that the centrifugal foam breaker was the most efficient to handle the rather large volume of foam that was formed. It consisted of a perforated plastic can attached to a variable speed stirrer that was adjusted to provide a reasonably constant flow of collapsed foam. The foam breaker was enclosed in a Lucite collection chamber closed by a lid in which openings were provided for the foam entrance and the stirrer. The collapsed foam was recycled by gravity flow through the recirculation line.

For the continuous runs, there was no need to break the foam since it was not recirculated, but to ensure the free flow of foam a thin coat of silicone grease applied around the foam outlet tube proved to be a very efficient foam breaker. Silicone grease, however, could not be used when the collapsed foam had to be recycled since it was not known if its presence in the solution resulting from solubilization or physical entrainment would affect its foaming characteristics.

All connections were made of Tygon tubing.

f. Photography

Bubble diameter measurements were made from photographs of the foam obtained with an Asahiflex camera with f = 50 mm lens, equipped with a bellows attachment, by using panatomic film 135ASA

(for fine-grained enlargement), with light being provided by floodlight (Superflood lamp No. 2). Measurement of the bubble size was accomplished by attaching a strip of graduated paper to the outer surface of the column. In spite of the fact that the scale and the bubbles lay on different planes, no correction for parallax was necessary, as evidenced by the perfect matching on a photograph of two scales attached on either side of the wall. There is apparently no distortion due to the curvature of the tube wall in the restricted picture region which was approximately 3 cm x 3 cm.

g. Surface Tensiometer

The surface tension of the EHDA-Br solutions was measured by a Cenco-Du Nouy Interfacial Tensiometer No. 70545 equipped with a platinum ring.

h. Analysis

Analysis for the concentration of bromide ion was performed to determine the concentration of the EHDA-Br solution. This was done by a potentiometric method using a glass and a silver electrode, with $AgNO_3$ as titrant (see Appendix B).

i. Surface-active Agent

Ethylhexadecyldimethylammonium bromide ($CH_3 (CH_2)_{15} (CH_3)_2 C_2H_5 N Br$), a quaternary ammonium salt and a cationic surfactant

was used in this study and was supplied by Eastman Organic Chemicals, Rochester, New York, U.S.A. (Catalog No. T5661).

2. Experimental Procedure

a. Surface tension measurements

The surface tension of aqueous solutions of EHDA-Br ranging in concentration from 0.004 to 1.0 g/l were measured. Measurements were made in an evaporating dish which had been cleaned with sulfochromic acid mixture and rinsed with the solution to be measured. The platinum ring was flamed before each measurement. Although no effort was made to maintain a constant temperature, the measurements were made in a short period in which the temperature of the solution was 79 $\pm$ 1°F. Four or five readings were averaged for each solution and reproducibility was within $\pm$ 0.3 dynes/cm.

b. Total Reflux Operation

Single-stage equilibrium studies were conducted with the 2 in. diameter column exclusively. Saturated air at a selected rate (adjusted by a valve and measured by a rotameter) was fed to the bubbler. The column was charged with 2 liters of an aqueous solution of EHDA-Br, the foam breaker was then started and the solution allowed to foam for at least 3 hours with all the foam produced being collapsed and recirculated.

At the end of each test, 2 or 3 photographs of the foam near the foam outlet were taken. The foam velocity and foam rate were determined from the time a bubble took to travel a distance of 10 or 20 cm between two lines drawn on the column. The collapsed foam rate needed to determine the liquid content of the foam (foam ratio) was obtained by volumetric timing of a small quantity of foamate (20 to 50 cc depending on the foam rate) at the end of each test. The collapsed foam and a sample of the bulk solution were titrated by the potentiometric method outlined in Appendix B.

c. Continuous Operation

For the continuous runs, the feed stream of concentration x_L was fed continuously to the column at a rate L measured by a calibrated rotameter. Foam and bulk liquid were also withdrawn continuously at the top and the bottom of the column respectively. The solution-foam interface was maintained at a constant level with some difficulty by adjusting the level of the exit line from the bottom of the column. Steady state was deemed to exist when all variables (foam velocity, foamate rate, bottoms rate, foamate concentration, bottoms concentration) became constant with time. Although preliminary tests had indicated that steady state was reached after about 2 hours, each test was carried out for at least 4 hours, with occasional checks on concentrations and

flow rates, to minimize small fluctuations in feed rate and liquid level. Foamate rate (F) and bottoms flow rate (B) were determined volumetrically by collecting these streams in graduated cylinders for 15 to 20 minutes.

d. Bubble Diameter Determination

The negatives of the photographs of the foam were magnified 20 to 25 times in a microfilm reader. Approximately 50 bubbles were measured which then permitted calculation of the average bubble diameter.

V RESULTS AND INTERPRETATION

1. Surface Tension of Aqueous Solutions of EHDA-Br

The surface tensions of aqueous solutions of EHDA-Br at 79 ± 1°F as determined by the Du Nouy ring tensiometer are listed in Table 1 and plotted in Figures 4 and 5.

Table 1

Surface Tension of Aqueous Solutions of EHDA-Br at 79 ± 1°F

Concentration of EHDA-Br g/l	Surface tension dynes/cm
0.000	71.8
0.004	68.6
0.010	67.7
0.0235	63.2
0.040	57.1
0.096	46.8
0.200	38.3
0.413	34.4
0.514	35.1
0.960	34.0
5.130	33.4

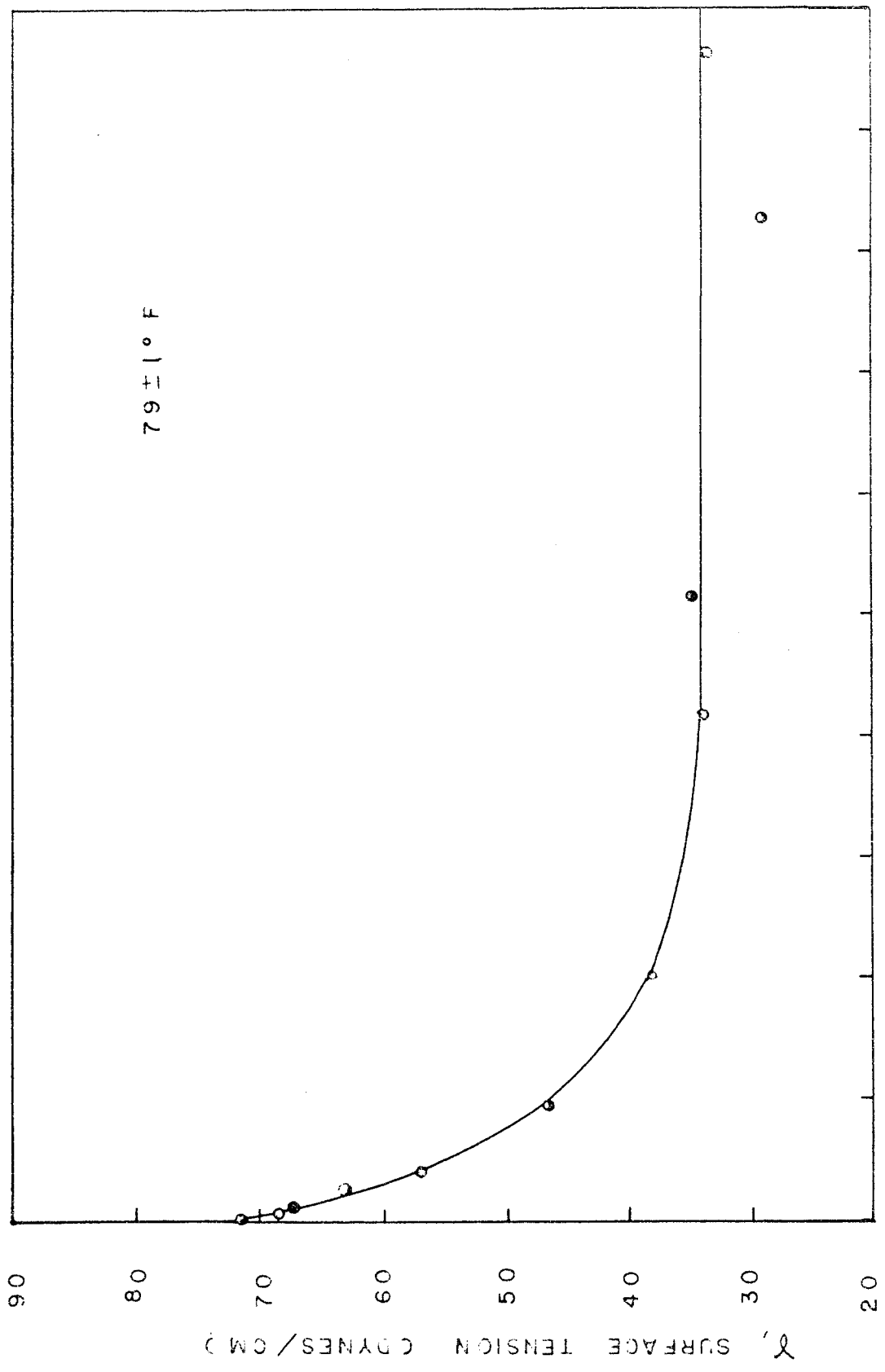

Figure 4. Surface tension of aqueous solutions of EHDA-Br

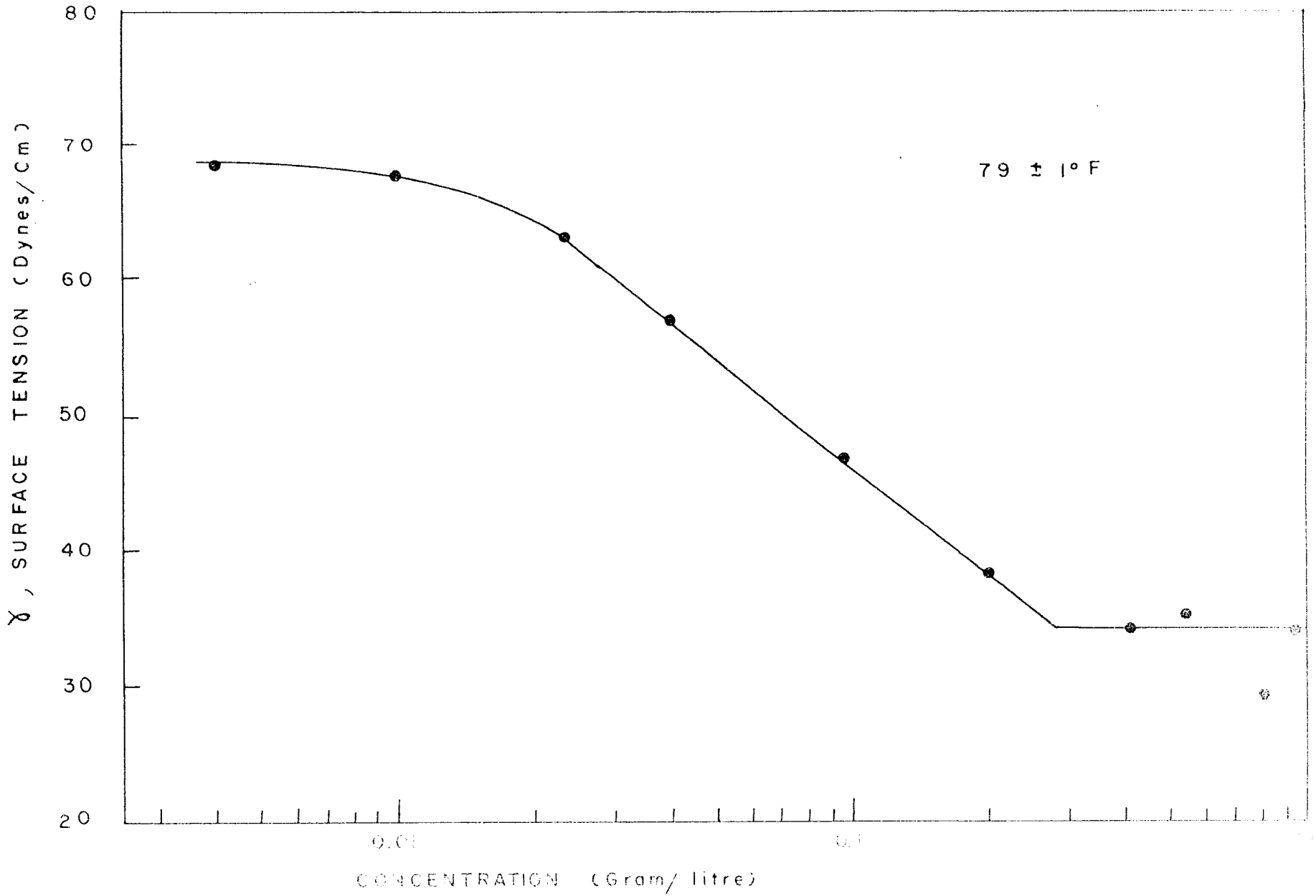

Figure 5. Surface tension of aqueous solutions of EHDA-Br

Figure 5 shows that the slope of the curve γ versus the logarithm of concentration is constant for concentrations ranging from 0.02 g/l to about 0.28 g/l and thus according to Gibbs' adsorption isotherm (equation 5) the surface excess Γ should be constant and independent of the concentration in this region.

The discontinuity in the curve of surface tension shows that the critical micelle concentration (c.m.c.) is about 0.28 g/l. Above that concentration, a new phase consisting of surfactant micelles is formed and Gibbs' equation cannot be applied since it does not contain any term accounting for the aggregation of molecules.

2. Single-stage Equilibrium Studies

a. Object

In the first part of this study, exploratory tests were conducted to assess the foaming ability of EHDA-Br. The effects of operating variables on the performance of a single-stage equilibrium column were also studied. Finally, the surface excess was determined at different foam rates and concentrations, and its value compared with values predicted by Gibbs' equation. The independent variable was chosen to be the foam rate G which is slightly different from the gas rate G' measured at STP conditions, due to the pressure drop across the bubbler. The

foam rate was chosen as the independent variable because it is directly related to the drainage time, i.e., the time a bubble spends in the foam column. For this part, experiments were conducted with the 2 in. diameter column and a 20 micron porous metal plate bubbler with all the collapsed foam being recirculated.

b. Foamability of EHDA-Br and Observations on the Structure of its Foam

EHDA-Br foams readily at almost any concentration. However, solutions below 0.1 g/l (0.01% weight) produce unstable foams with a tendency to break in the foam column and to cover the wall of the column with a blanket of stationary bubbles.

During the course of this work, two extreme types of foams have been observed (Figures 6a and 6b):

(a) Wet foams with spherical bubbles and a high liquid content

(b) Dry foams with polyhedral bubble and a low liquid content.

In general, the bubbles are reasonably spherical, except at very low foam rates (i.e. low foam velocity). At these low foam rates, coalescence occurs at the top of the column, producing polyhedral bubbles. Since the equations in chapter III are derived on the basis of the absence of coalescence, data with coalescent bubbles must be rejected. Furthermore, if the foam is stable but not spherical the

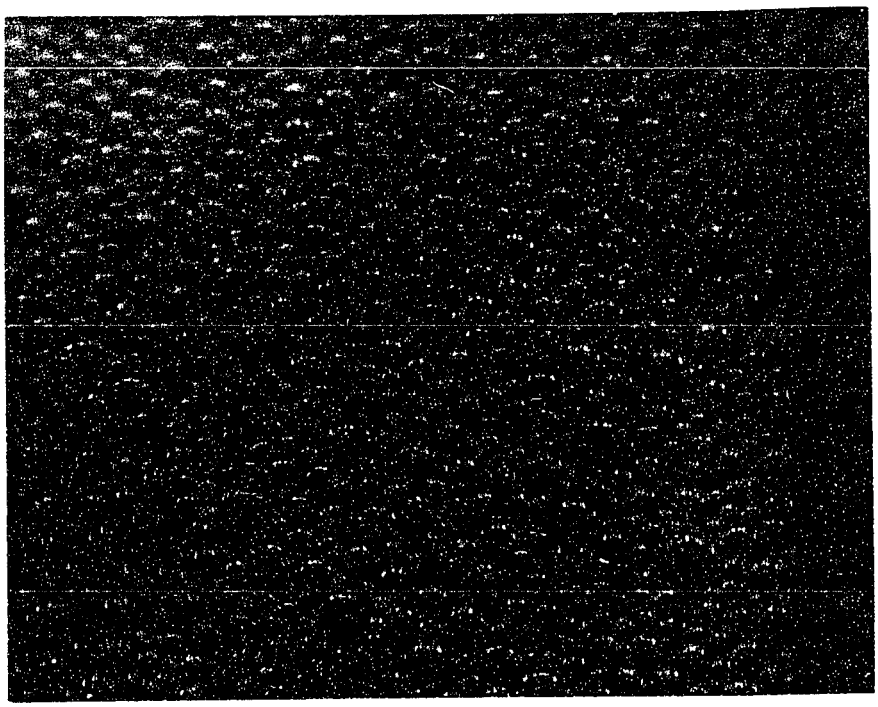

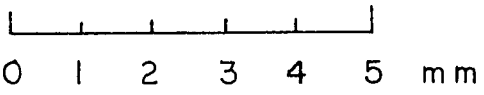

Figure 6a. Example of a wet foam

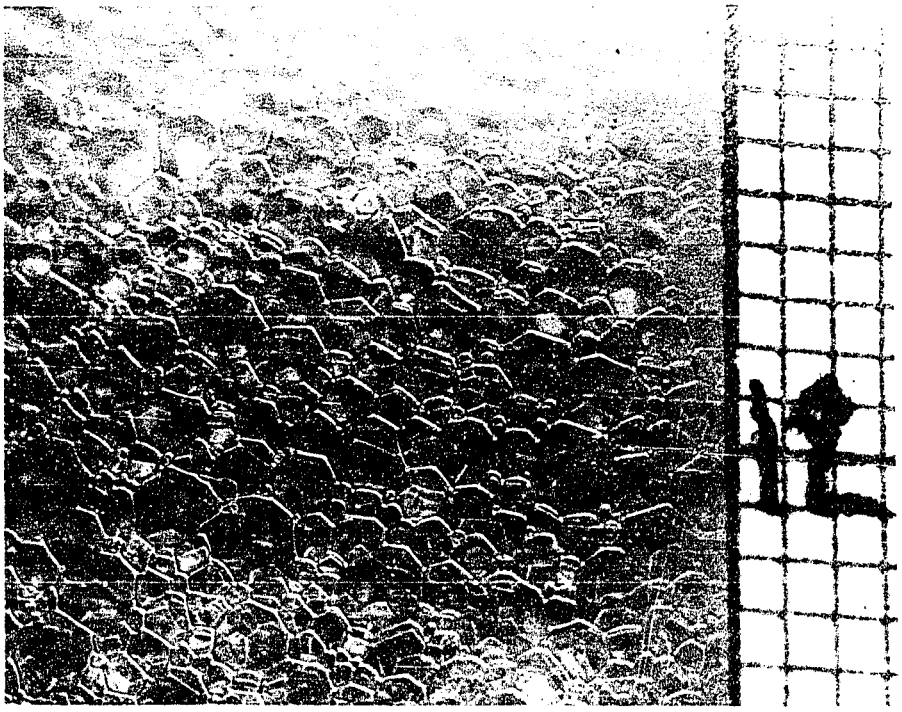

0 1 2 3 4 5 mm

Figure 6b. Example of a dry foam

factor 6 in equation (11) has to be changed to take into account the shape of the bubbles.

c. Variation of the Diameter of Bubbles with Distance from the Interface

A series of photographs taken at various points above the solution-foam interface showed that the size of bubbles was not constant throughout the foam columns. Typical results are reported in Table 2 and plotted in Figure 7.

Table 2

Variation of Bubble Diameter with Distance from Interface

x_B = 0.305 g/l

Foam rate = 593 cc/min

Distance from interface (cm)	D (mm)
7.0	0.85
26.5	0.87
42.5	0.89
63.5	0.98
65.0	0.95

x_B = 0.294 g/l

Foam rate = 520 cc/min

Distance from interface (cm)	D (mm)
0	0.72
14.5	0.75
34.0	0.84
52.0	0.88
60.0	0.92
61.5	0.91

Drainage occuring in the foam column was accompanied by thinning of the bubble walls. In the case of stable foam, the diameter of the bubbles therefore increased with the time allowed for drainage. Since the significant variable in this case is the time a bubble stayed in

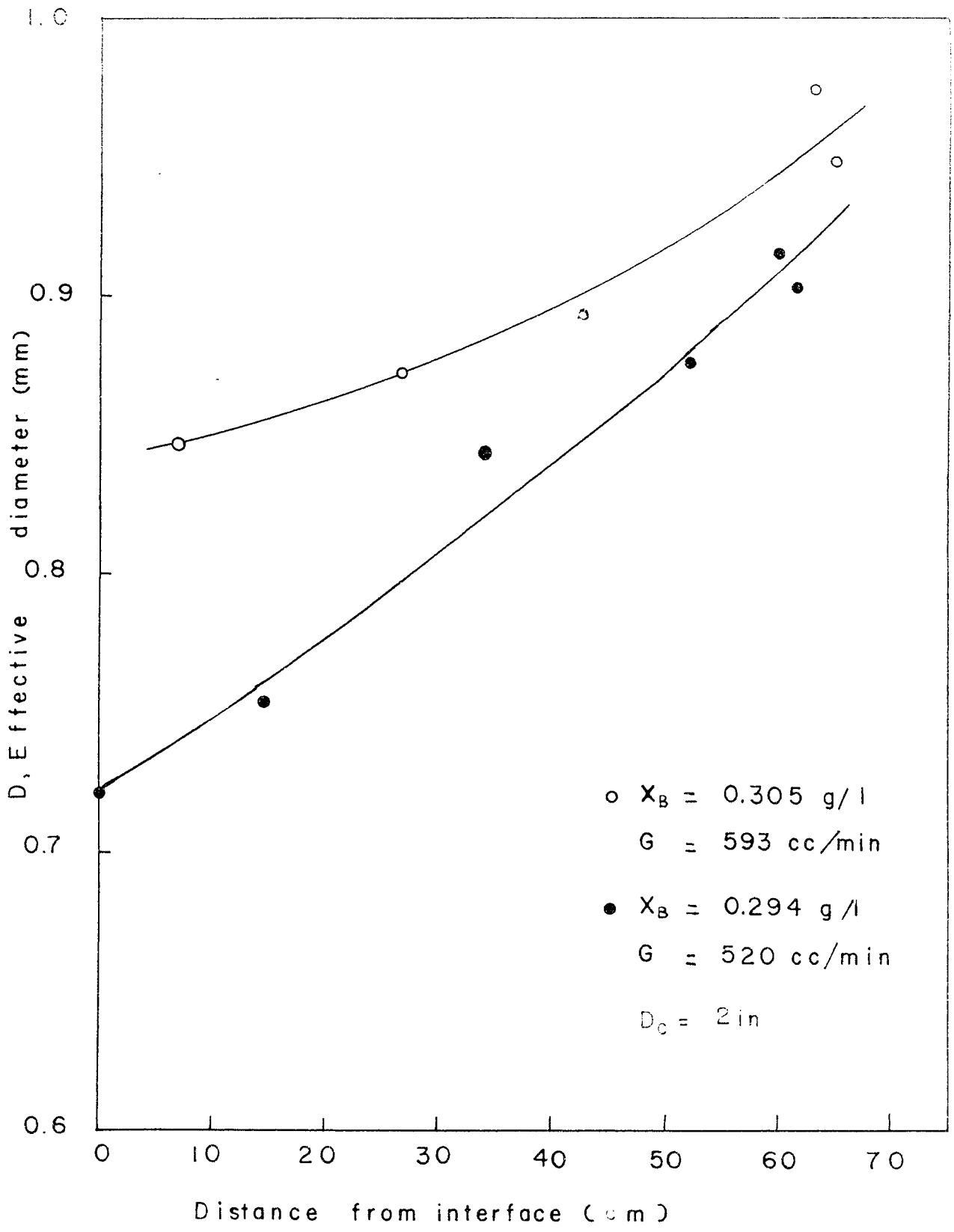

Figure 7. Variation of bubble diameter with distance from interface

the foam column, the rate of increase in diameter with distance from the interface was greater at lower foam velocity as demonstrated by Figure 7. In subsequent calculations, the effective diameter was determined from photographs taken near the outlet of the foam column, since all other characteristics (liquid content, concentration , etc...) are determined for the foam at the outlet.

In view of its important influence on the performance of foam separation columns, the drainage of solution between foam bubbles has been studied extensively. Miles et al (46) have treated foam as a series of capillary tubes. Jacobi et al (47) considered foam drainage as liquid flowing between parallel plates. Haas and Johnson (48) arrived at semi-empirical relations by assuming a flow through Plateau borders of curved triangular cross-section with non-rigid boundaries. More recently Leonard and Lemlich (49) proposed a model involving the flow through randomly oriented capillaries (Plateau borders) of non circular cross-section with finite surface viscosity at its boundaries. The model was experimentally verified by Fanlo (50) with the system Triton-X-Water. None of these studies have been concerned with the expansion of the bubbles but this phenomenon has been studied qualitatively and quantitatively by Mysels and his co-workers (49, 51).

d. Effect of Foam Rate on Enrichment and Foam Ratios

The effect of foam rate on enrichment ratio and foam ratio has been studied for 3 different concentrations: 0.15 g/l, 0.20 g/l, 0.30 g/l. In Figures 8 to 10, the enrichment ratio and foam ratio are plotted against foam rate. It is seen that the enrichment ratio decreased and the foam ratio increased with increasing foam rate. This is understandable since increasing foam rate means more liquid entrained with the bubbles, thus increasing the liquid content and decreasing the concentration of the foam and consequently the enrichment ratio. At high foam rates the rate of decrease of the enrichment ratio with increasing foam rate decreased sharply and at very high gas rates E would tend to unity since the intersticial liquid in the foam will be almost entirely entrained liquid from the bulk solution. It can be seen that very high enrichment ratios can be obtained by lowering the foam rate but the foam will be very dry and unstable.

e. Surface Adsorption

The surface excess was calculated from foam separation data and compared with the theoretical value obtained from Gibbs' equation and surface tension data.

i. Surface excess from surface tension data

From equation (5) and surface tension data:

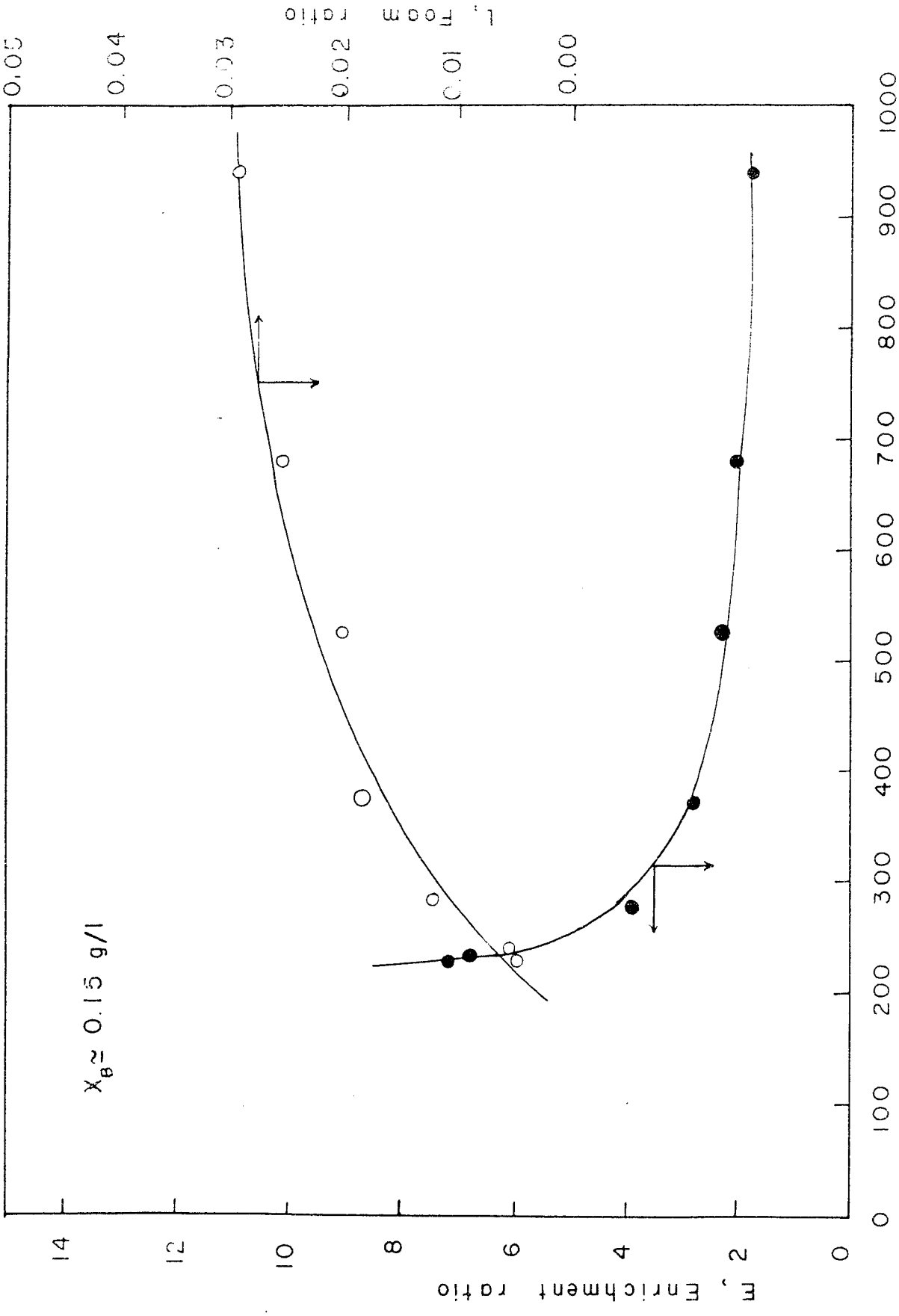

Figure 8. Effect of foam rate on enrichment and foam ratios

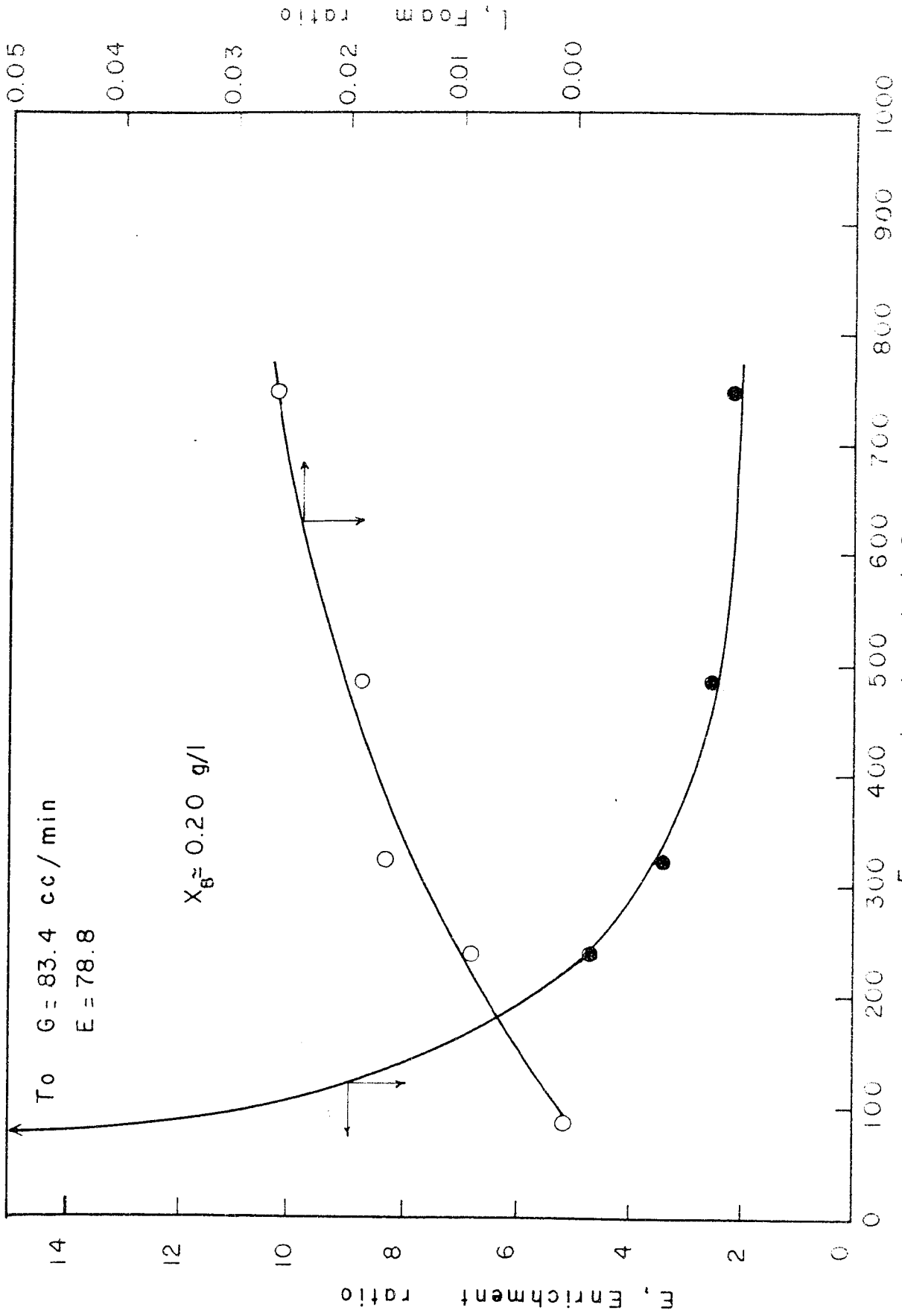

Figure 9. Effect of foam rate on enrichment and foam ratios

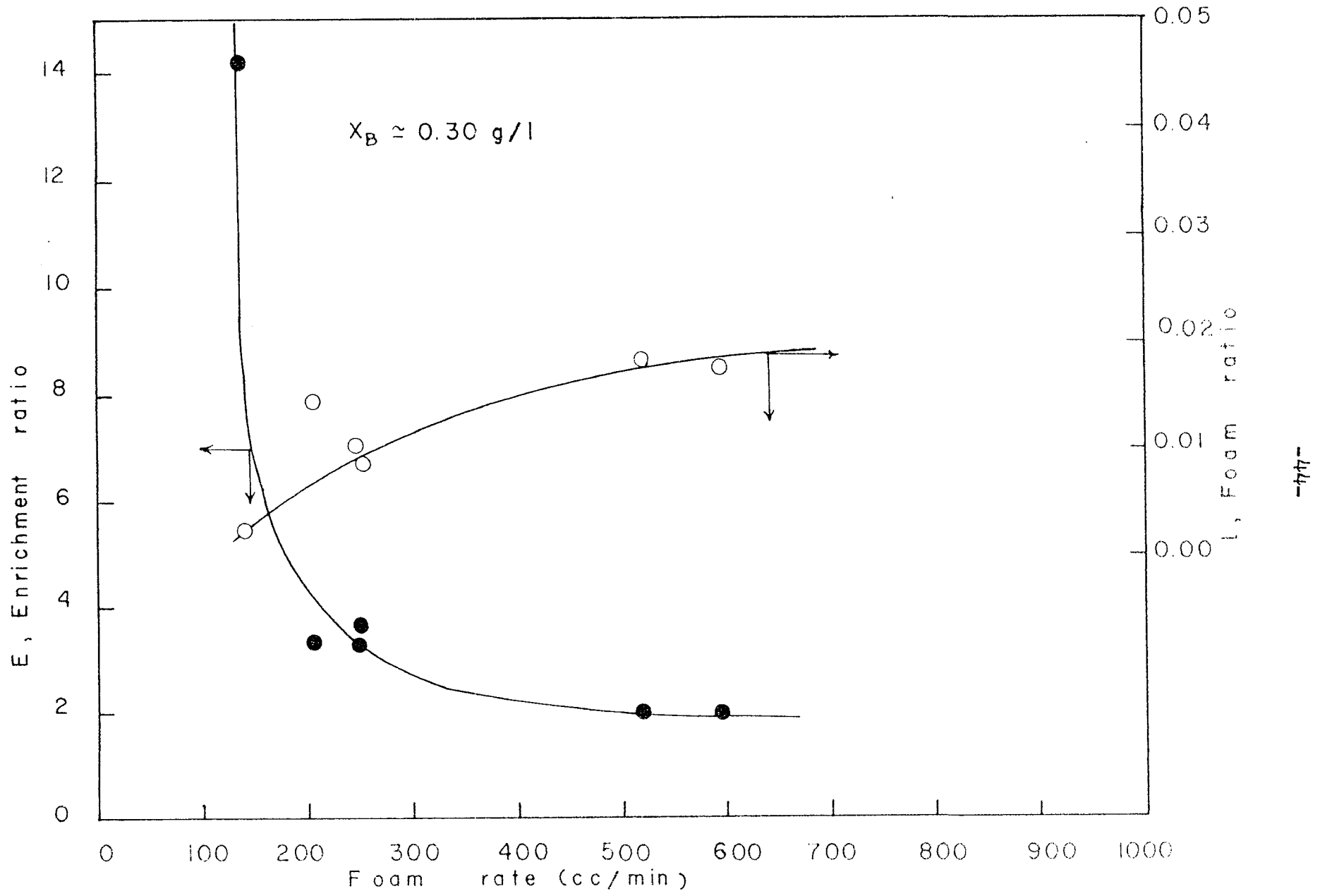

Figure 10. Effect of foam rate on enrichment and foam ratios

$$\Gamma = -\frac{1}{2RT}\,\frac{d\gamma}{d\ln x_B} \qquad (5)$$

where $\frac{d\gamma}{d\ln x_B}$ = slope of Figure 5
= - 11.32 dynes/cm

According to equation (5), the value of Gibbs' surface excess is between 0.870×10^{-7} and 0.856×10^{-7} g/cm^2 for the 23° - 28° C temperature range.

If it is assumed that the interfacial phase consists of a monomolecular layer, the area of the EHDA-Br molecule would then be (taking the average value for Γ) 72.8 Å^2.

ii. Surface excess from foam separation data

The experimental value of surface excess Γ_{exp} was calculated from foam separation data and equation (15). The values of Γ_{exp} are listed on Table 3 and plotted against foam rate in Figure 11 with bulk concentration as the parameter. Figure 11 shows that:

(1) The experimental value of surface excess was not constant as would be expected by Gibbs' equation but varied with both foam rate and bulk concentration.

(2) Γ_{exp} decreased with increasing foam rate, reached a minimum value and then increased with increasing foam rate. This behaviour of Γ_{exp}

Table 3

Surface Excess from Foam Separation with Recycling Data

Final bulk concentration x_B (g/l)	Foam Rate cc/min	Γ_{exp} (g/cm^2) x 10^8
0.146	230.4	6.20
0.151	237.0	8.14
0.149	282.0	6.94
0.145	373.8	7.28
0.152	525.6	6.15
0.147	681.0	7.10
0.152	937.8	8.49
0.199	83.4	12.75
0.181	240.6	9.28
0.197	325.2	8.00
0.191	486.6	7.25
0.200	748.2	9.28
0.299	138.6	13.90
0.307	204.0	12.75
0.298	252.6	10.89
0.297	253.2	11.23
0.294	521.4	9.83
0.319	593.4	10.03

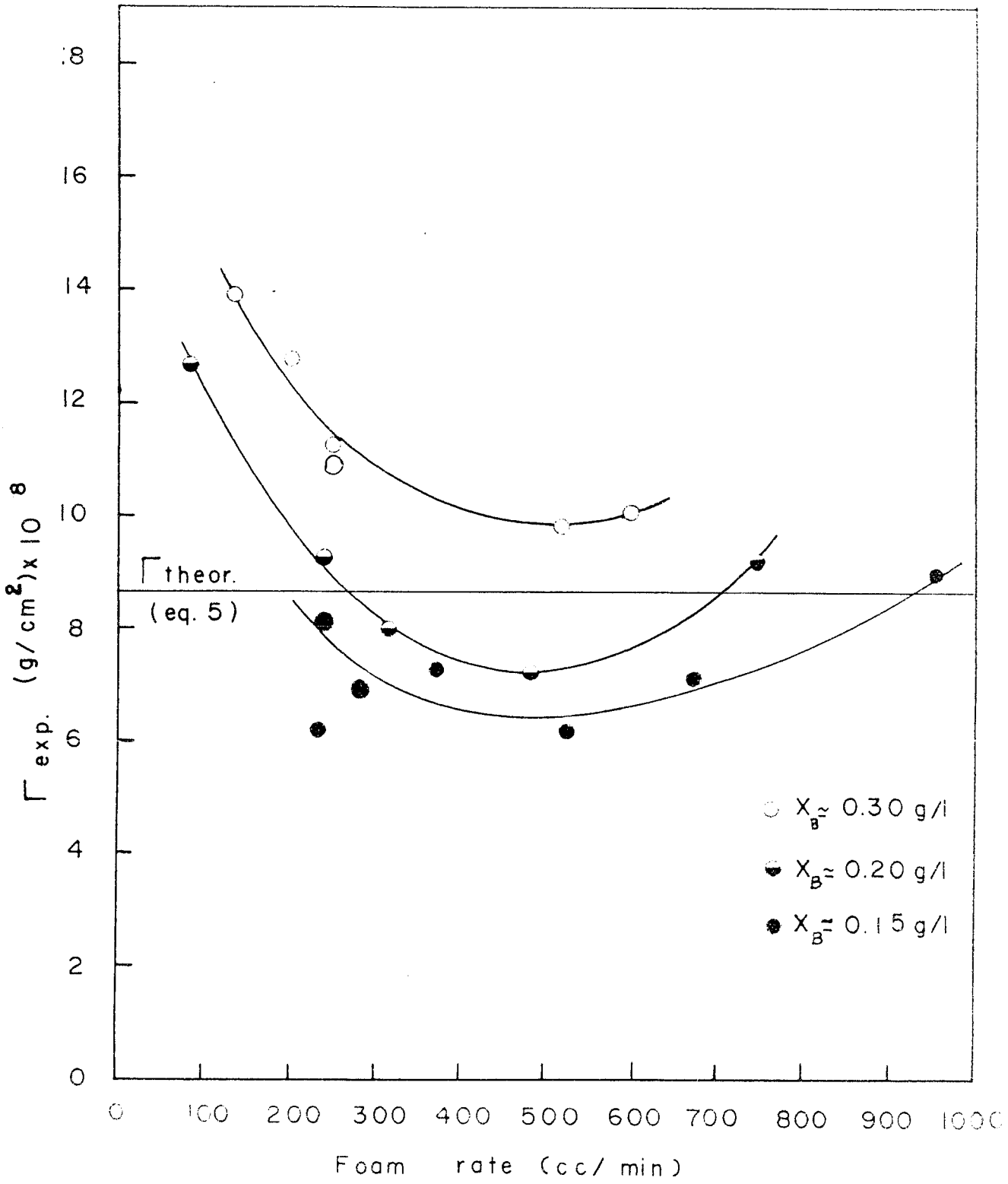

Figure II. Surface excess of EHDA-Br from foam separation with recycling data

with respect to foam rate was also observed by Kevorkian (43) with Aresket-300, an anionic surfactant, but his values of Γ_{exp} were always higher than the value obtained from Gibbs' equation and surface tension data. The behaviour of Γ_{exp} with respect to foam rate was likely due to two effects. At low foam rates, an increase in the foam rate caused more bulk liquid to be entrained with the bubbles. Since the entrained liquid was of a much lower concentration than the interfacial layer itself, the entrainment effectively reduced the concentration of the collapsed foam, giving a lower value of Γ_{exp}. At very low foam rates, the foam was given ample opportunity to drain and as a result the foam became very dry and the bubbles were no longer spherically shaped. To compensate for this, the numerical constant in equation (15) should be somewhat larger since the area of a polyhedron is larger than the area of a sphere occupying the same volume. Since the constant was taken as 6, Γ_{exp} as calculated by equation (15) was probably larger than its actual value. The situation was further complicated by the fact that, although the foam was fairly stable, breakage might occur at too low foam rates, providing internal reflux and increasing the value of Γ_{exp} since the system represented by the liquid pool and the foam column was no longer a single equilibrium stage. As the foam rate was increased, the entrainment effect probably reached a maximum beyond which it was

no longer the predominant factor. At high foam rates, the velocity of the gas may have caused the breakage of the bubbles, providing internal reflux which contributed greatly to the increase in the concentration of the foam and thus accounting for the increase in Γ_{exp}.

Comparison with the theoretical value of Γ as predicted by Gibbs' equation from surface tension data shows that for values of x_B below the c.m.c., Γ_{exp} was lower than predicted, except for very high and very low foam rates. A lower value is to be expected because of the entrainment (dilution) effect. It is likely that under "ideal" circumstances (i.e. no coalescence of the bubbles), Γ_{exp} would be expected to tend toward the predicted value at very low foam rates, since Gibbs' equation applies to static systems. The fact that Γ_{exp} was greater than $\Gamma_{theor.}$ at low and high foam rates simply indicates coalescence and breakage of the foam. It is believed that the application of Gibbs' equation to non-static system is somewhat doubtful. Furthermore, the extent of surface hydrolysis, and preferential adsorption of OH^-, in which case the theoretical value of Γ is twice the "normal" value of Γ, is not accurately known. The actual value of Γ_{exp} could be somewhat higher than the measured values since the concentration of $EHDA^+$ ion in the interfacial phase was measured for in its bromide form, and thus $EHDA^+$ in its hydroxide form produced by surface hydrolysis was not determined.

However, the order of magnitude of Γ_{exp}, which is quite reasonable compared to the surface excess calculated from equation (5) seems to indicate that surface hydrolysis is indeed negligible.

According to the surface tension-concentration curve, $x_B \simeq$ 0.30 g/l is above the c.m.c., and therefore Gibbs' equation cannot be applied, since it contains no term descriptive of the micelles. This is obviously so since Gibbs' equation would predict a zero surface excess whereas experimental results show a definite positive adsorption, even greater than with solutions below the c.m.c. It has been reported by Wilson et al (52) and Kishimoto (13), that the surface excess remains constant above the c.m.c., although no explanation, qualitative or otherwise, has been offered. It must be emphasized that just because the experimental values of Γ do not agree with the predicted values, this does not question the validity of Gibbs' equation since it was derived for static interfaces. The absence of information on the extent of ionization and hydrolysis of the surfactant makes any meaningful comparison very difficult, as does the uncertainty in the determination of an effective diameter of non spherical and non uniform bubbles.

iii. Review of attempts to verify Gibbs' equation experimentally

The amount of adsorbed material is usually so small that its experimental determination and consequently, an experimental confir-

mation of Gibbs' equation could not be achieved for many years. The rising bubble technique has been employed by McBain and co-workers (53, 54) to measure adsorption of aqueous solutions of isoamyl alcohol, acetic, butyric, caproic, nonylic acids, phenol, p-toluidine, resorcinol, thymol, camphor, Na Cl. They found that 2 to 8 times as much solute was carried along by the bubbles as would be predicted by Gibbs' equation. However, McBain (55), using an elaborate apparatus to skim off a very thin layer of static air-solution interfaces of phenol, caproic acid, p-toluidine, found good agreement with Gibbs' equation. Kishimoto (13), using data of Wilson et al (52) and assuming complete dissociation of the electrolyte, obtained very good agreement with Gibbs' equation for sodium lauryl sulfate and noted that surface excess remains constant above the c.m.c. This is remarkable, since Wilson's data were obtained from direct foam separation with recycling data. Lemlich (44) claimed an agreement within 10% for the system Aresket-300-Water from foam separation data, but he used equation (6) without justifying it. Dixon et al (56), using radiotracers on Aerosol OTN, an anionic surface-active agent, found fair agreement with Gibbs' equation by assuming that the undissociated form of that organic electrolyte is more strongly adsorbed than its ion.

In conclusion, it appears that:

(1) Gibbs' equation gives only approximate information with regard

to surface concentration. This is due to the formation of ion pairs and possibly small micelles even at concentrations below the c.m.c.

(2) The usefulness of Gibbs' equation is limited by the lack of information on the extent of surface hydrolysis which occur, even with strong electrolytes.

(3) Above the c.m.c., multilayer adsorption is possible.

2. Continuous Foam Separation of EHDA-Br

a. The Ideal Foam Model

In order to verify the assumptions involved in the ideal foam model, $(y_F - x_B)$ DF, $(x_L - x_B)$ DL, $(y_F - x_L) \frac{DFL}{B}$ have been plotted in Figure 12 against foam rate (G). If equations (20 - 22) based on the ideal foam model are to be satisfied, the plot should yield a straight line with slope $\frac{-3}{RT} \frac{d\gamma}{d \ln x_B}$. The ordinate Y* represents the average value of $(y_F - x_B)$ DF, $(x_L - x_B)$ DL, $(y_F - x_L) \frac{DFL}{B}$ with vertical lines drawn through the points to indicate deviations from the average values. The data were obtained from continuous runs with the 2 in. diameter column, a 20 micron porous metal bubbler, at a feed rate of 52 ± 2 cc/min and for 3 feed concentrations: 0.15, 0.20, 0.30 g/l. Examination of Figure 12 shows that at high foam rates, the values of Y* are consistently below the theoretical values predicted by equations (20 - 22), whereas at low foam

Table 4

Surface Excess from Continuous Foam Separation Data

x_L (g/l)	G (cc/min)	x_B (g/l)	$(y_F - x_B)$ FD (g - cm)/min $\times 10^4$	$(x_L - x_B)$ LD (g - cm)/min $\times 10^4$	$(y_F - x_L)\frac{LFD}{B}$ (g - cm)/min $\times 10^4$	Y* avg (g - cm)/min $\times 10^4$	Γ_F (g/cm^2) $\times 10^8$	Γ_B (g/cm^2) $\times 10^8$
0.150	91.4	0.140	0.690	0.639	0.675	0.668	12.55	11.65
0.151	121.6	0.125	1.392	1.380	1.375	1.382	19.08	18.90
0.151	192.0	0.122	1.492	1.350	1.399	1.414	12.85	11.75
0.149	271.4	0.114	1.400	1.560	1.396	1.425	9.26	9.42
0.150	503.2	0.098	2.337	2.270	2.133	2.247	7.74	7.51
0.202	93.5	0.178	1.759	1.352	1.747	1.619	31.26	24.13
0.200	187.1	0.168	1.006	1.350	0.995	1.177	9.11	7.34
0.202	265.1	0.155	1.403	1.565	1.380	1.449	8.84	9.84
0.203	289.4	0.162	1.597	1.600	1.593	1.596	9.19	9.10
0.202	453.6	0.139	1.819	2.088	1.560	1.822	10.12	7.68
0.202	629.9	0.130	2.100	2.630	1.620	2.117	5.59	6.97
0.202	683.1	0.124	2.877	2.850	2.927	2.885	7.38	6.95
0.200	800.8	0.127	2.794	3.165	2.265	2.741	5.83	6.58
0.202	942.0	0.090	5.040	5.040	-	5.040	8.91	8.77

Table 4 (Continued)

x_L (g/l)	G (cc/min)	x_B (g/l)	$(y_F - x_B)FD$ (g - cm)/min $\times 10^4$	$(x_L - x_B)LD$ (g - cm)/min $\times 10^4$	$(y_F - x_L)\frac{LFD}{B}$ (g - cm)/min $\times 10^4$	Y* avg (g - cm)/min	Γ_F (g/cm^2) $\times 10^8$	Γ_B (g/cm^2) $\times 10^8$
0.303	130.7	0.265	1.195	1.295	1.180	1.223	15.24	16.57
0.301	207.5	0.246	1.386	1.394	1.629	1.469	9.57	9.54
0.303	356.0	0.229	1.466	1.815	1.220	1.500	6.86	8.49
0.301	435.8	0.212	1.902	1.900	1.897	1.899	7.27	7.28
0.302	514.0	0.202	2.449	2.402	2.449	2.433	7.93	7.78
0.301	529.0	0.205	2.627	2.670	2.557	2.618	8.29	8.28

L = 52 ± 2 cc/min

D_c = 2 in.

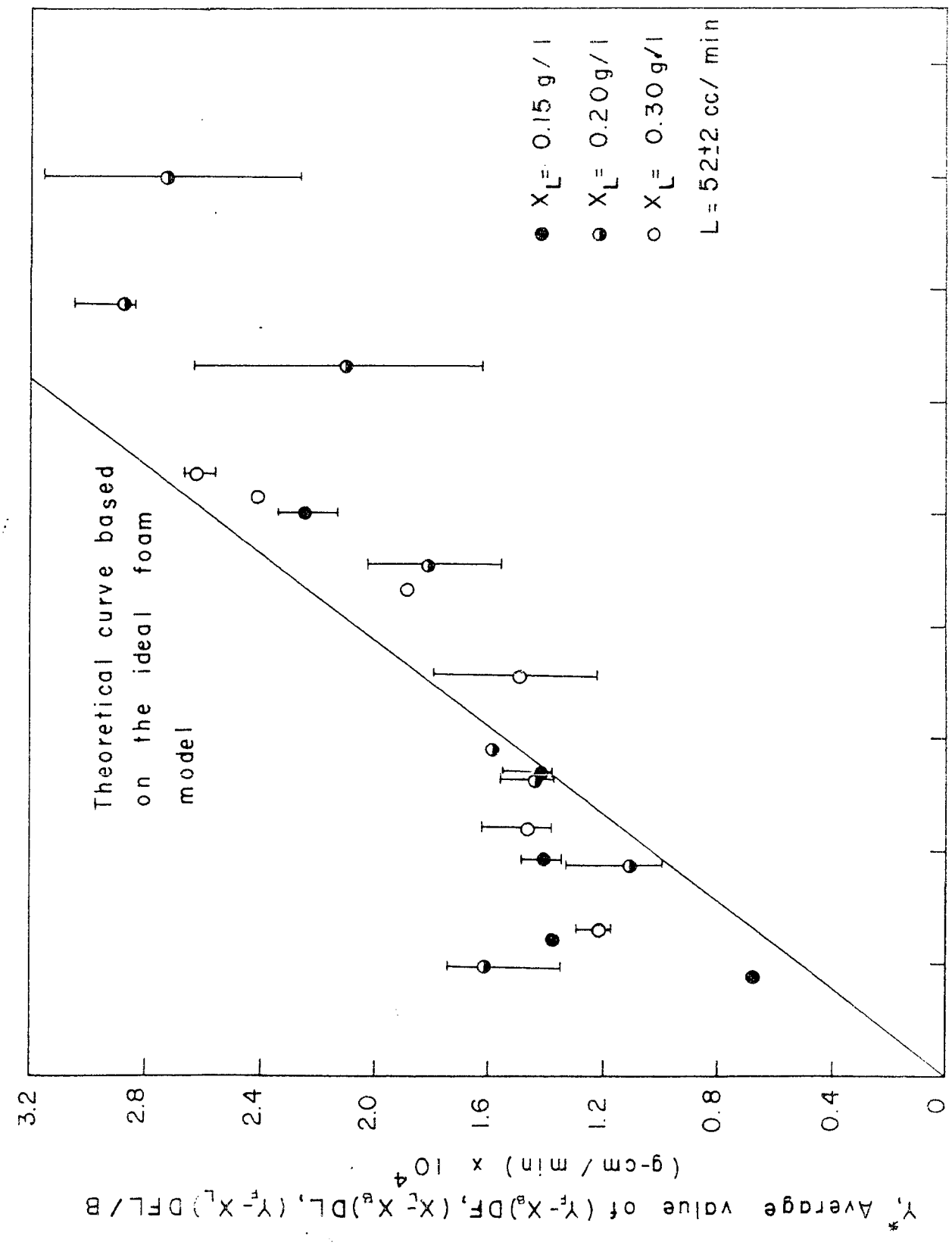

Figure 12. Verification of the ideal foam model

rates (below 300 cc/min), Y* is consistently above the theoretical values. This indicates that at low foam rates coalescence and breakage of bubbles occured, thereby providing internal reflux and the system consisting of the liquid pool and the foam column could no longer be considered to be a single equilibrium stage. Despite the scattering of data, there was no indication of any dependence of Y* on x_L and consequently on x_B.

b. Surface Excess from Continuous Foam Separation Data

The surface excess values calculated from equations (23) and (24) are listed on Table 4 and are plotted in Figure 13. The values of Γ_B and Γ_F show reasonable consistency. The deviation from the average value of Γ is not greater than 15% and in 70% of the cases, it is less than 5%. The behaviour of Γ with respect to foam rate was similar to that observed with total reflux data. But in this case, it is difficult to ascertain the dependence of Γ with bulk concentration since the parameter is feed concentration. Dependence of Γ upon concentration, if there is any, was probably masked by the inherent nature of the experimental data. Between foam rates of 200 and 950 cc/min experimental values of Γ were consistently lower than the value predicted by Gibbs' equation, although the deviations from the theoretical value never exceeded 30%. As the foam rate decreased, Γ increased rapidly, reaching values

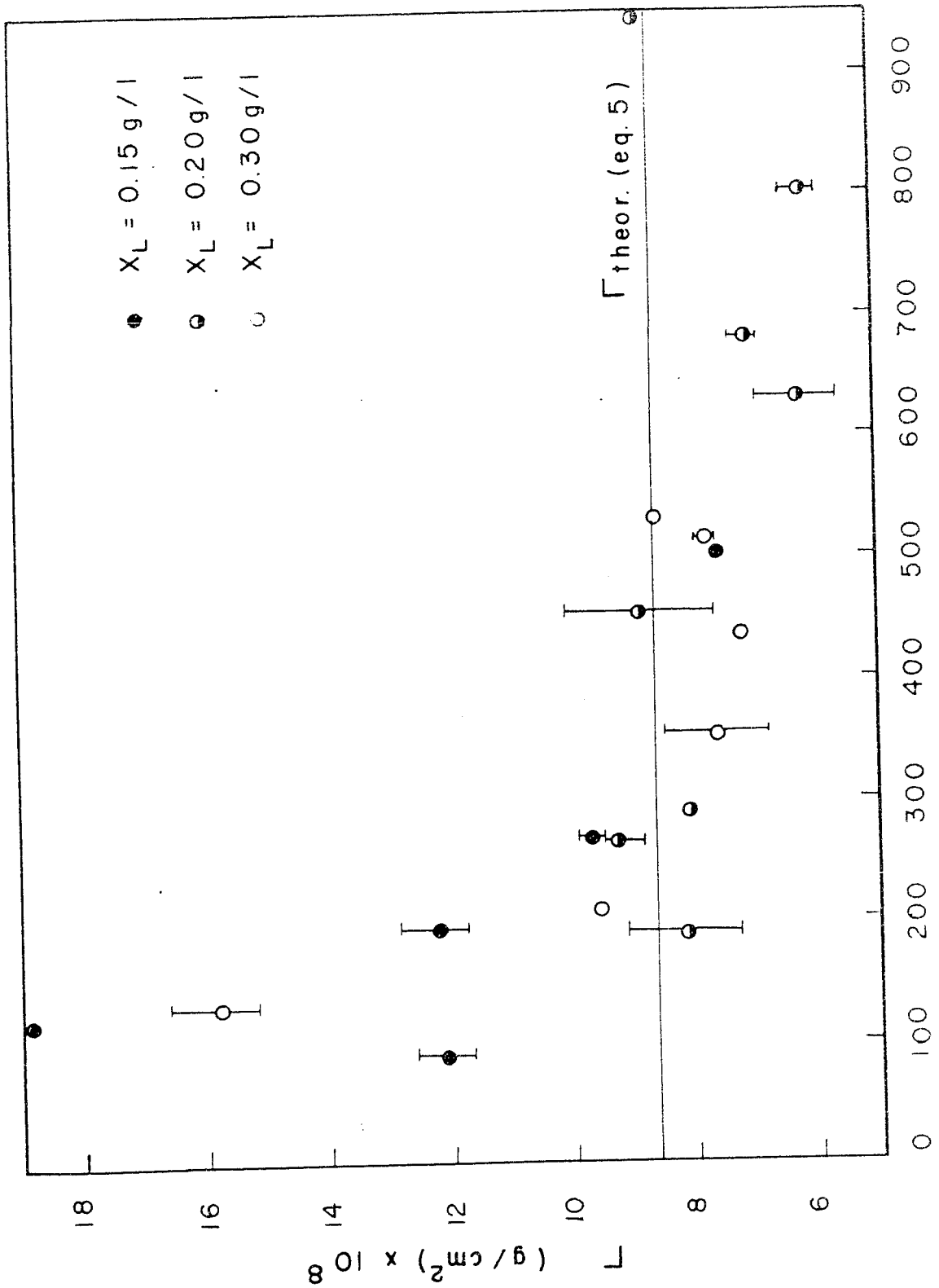

Figure 13. Surface excess of EHDA-Br from continuous foam separation data

several times greater than the theoretical value. As in the case of total reflux, drainage, bubble coalescence and internal reflux were presumably responsible for the exceedingly high values of Γ_{exp}.

c. Conclusion: Validity of the Ideal Foam Model

In order to appreciate the applicability of the ideal foam model to the foam separation process, the validity of the assumptions involved in the derivation of equations (20 - 22) must be assessed.

(1) The assumption of a completely mixed liquid pool would be expected to be valid in view of the stirring effect of the bubbles, and in fact this has been verified by Grieves and Wood (23).

(2) Experiments conducted with different foam heights (see under: effect of foam height) showed that for a foam column high enough to ensure good drainage and at a constant gas rate and feed rate, there was no variation in x_B although y_F increased with increasing foam height, indicating that most of the entrained liquid is of the same concentration as the bulk liquid.

(3) The condition of complete stability of the foam is not likely to be met at extreme conditions, i.e., at either very low or very high foam rates. At very low foam rates, coalescence of bubbles occurred, producing polyhedron-shaped bubbles, the surface area of which was

difficult to measure with accuracy. At very low and very high foam rates, breakage of the foam due to excessive thinning of the bubble walls and to the gas velocity produced internal reflux.

(4) The most critical assumption employed stated that the interfacial layer was in equilibrium with entrained liquid which was assumed to be of the same concentration as the liquid pool. This means that y_S is the concentration that would be achieved after an infinitely long period of contact and is related to x_B by some equilibrium function, e.g., Gibbs' equation. Thus the whole column is considered as a single equilibrium stage. Any increase in the concentration of the foam phase would then be due only to drainage and not to mass transfer. However restricting this assumption may appear it is justified, provided no bubble breakage occurs which liberates the gas phase and brings it into contact with a richer liquid phase, that is, there should be no internal reflux.

(5) The last assumption, namely that Gibbs' equation applies to non-static interfaces may or may not be justified, depending perhaps on the nature of the surfactant. It seems to be applicable to EHDA-Br provided all the factors governing its adsorption at solution air interfaces are taken into account.

Under ideal circumstances, i.e., with foams stable enough to produce spherical bubbles which remain unbroken at very low foam velocities to ensure quasi-static conditions, equation (21) can be used to predict x_B, provided bubble diameter is known with reasonable accuracy.

d. Importance of Operating Variables

In order to evaluate foam fractionation as a feasible chemical engineering separation technique, a large volume of information is required on the factors which control the separation.

The important dependent variables in a continuous operation are:

(1) Separation efficiency, expressed as "Enrichment Ratio" ($E = y_F/x_B$), or "Stripping Ratio" ($S_R = x_B/x_L$). The enrichment ratio is to be maximized in an enriching operation (e.g. recovery of valuable metal ions) and the stripping ratio to be minimized in a decontamination operation (e.g., decontamination of waste streams). These parameters, however, do not give any information concerning the foam rate and the stripped effluent rate.

(2) Effluent and overhead rates expressed as volume ratios F/L and B/L, or as "Volume Split" F/B. It is generally desirable to minimize

the volume split.

(3) The "Removal Ratio" Fy_F/Lx_L, which measures the percentage of surfactant removed from the feed. It is desirable to maximize this parameter.

The effects of different operating variables on these parameters and also their importance relative to one another is the information needed in the design and operation of a foam separation unit giving the greatest enrichment at the lowest unit cost.

e. Effect of Operating Variables

i. Bubble Diameter

(1) Effect of Foam Rate on Bubble Diameter

The effective bubble diameters determined from photographs of the foam and equation (9) are plotted against foam rate in Figure 14, with feed concentration as the parameter. The data were obtained with the 2 in. column and the 20 micron porous metal gas sparger at a feed rate of 52 ± 2 cc/min. Since Figure 14 shows that bubble diameter passed through a minimum with increasing foam rate, it would appear that bubble diameter was determined by the interaction of two effects:

(1) Gas rate, the increase of which normally produced larger bubbles since a larger volume of gas passed through the pores of the sparger.

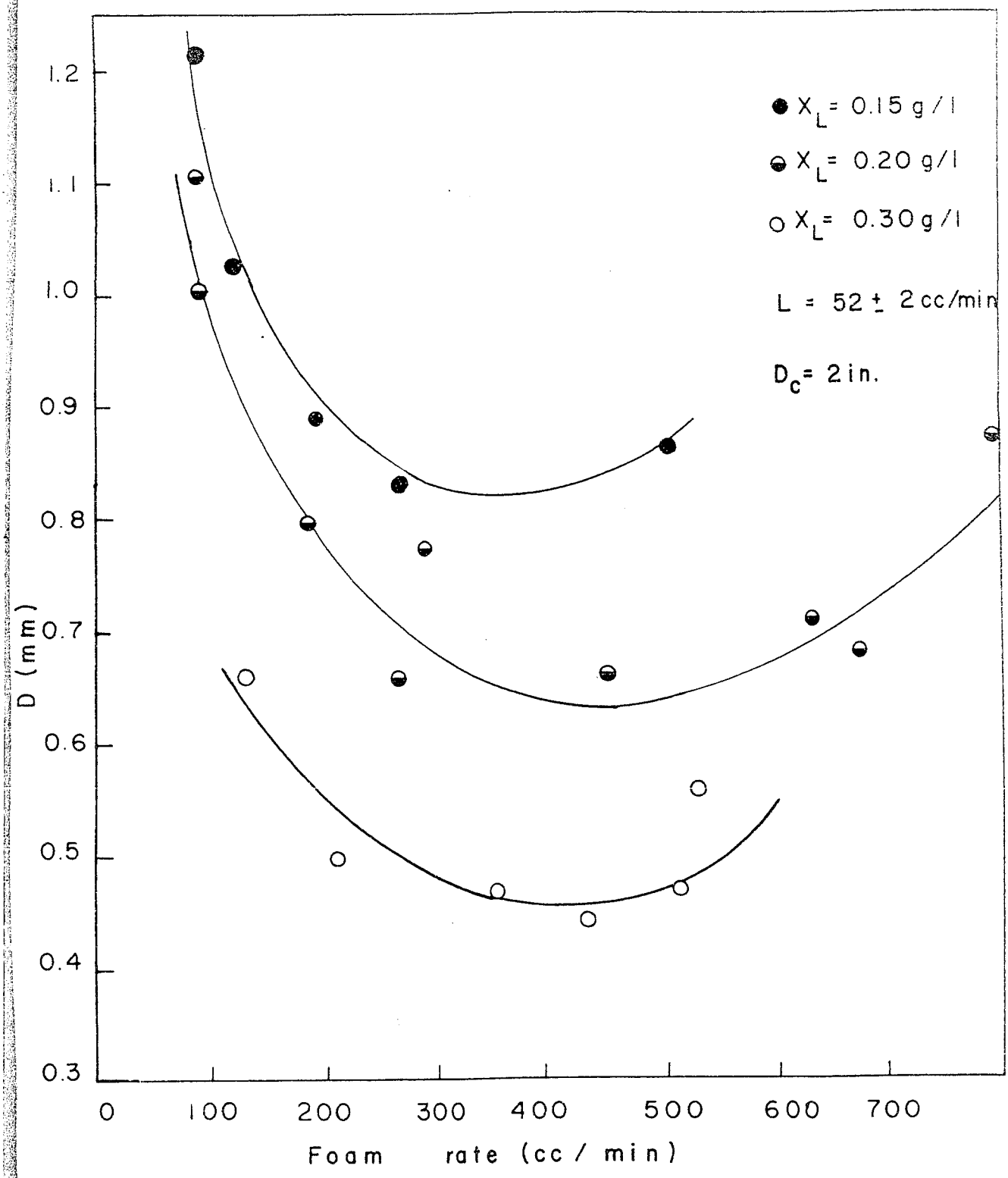

Figure 14. Variation of bubble diameter with foam rate

(2) The drainage effect, that is, a lower foam rate means a lower velocity of the bubbles and consequently more opportunity for drainage and thinning. At very low foam rates, the foam was very dry and coalescence might even occur, increasing appreciably the diameter of the bubbles. The fact that the minimum seems to occur at the same foam rate (around 400 cc/min) independent of x_L indicates that the thinning of bubble walls is independent of concentration.

2. Effect of Feed Concentration on Bubble Diameter

Figure 14 also shows that for the same foam rate, bubble diameter decreases with increasing feed concentration although bubble diameter probably depends on the bulk concentration x_B rather than the feed concentration x_L, but since x_B decreases with decreasing x_L for the same foam rate, the effect is the same. The dependence of bubble diameter with concentration can be explained by considering that when a bubble forms slowly at an orifice, it will detach and rise through the solution when the buoyant force is just greater than the force due to surface tension acting along the perimeter of the orifice. This can be stated quantitatively to be when

$$\frac{\pi D^3}{6} g (\rho_l - \rho_g) = \pi D' \gamma \qquad (25)$$

where D = bubble diameter

g = acceleration of gravity

ρ_l = density of liquid

ρ_g = density of gas in the bubble

D' = orifice diameter

γ = surface tension of solution

$$D = \left[\frac{6 D'}{g (\rho_l - \rho_g)} \right]^{1/3} \gamma^{1/3} \qquad (26)$$

Since the surface tension decreases with increasing concentration, it is seen from the above equation that D also decreases. Equation (26) cannot be used directly to determine the bubble diameter since it is derived for bubbles forming very slowly, with buoyancy force in equilibrium with surface tension. It does show, however, the dependence of bubble diameter upon concentration.

ii. Effect of Feed Concentration

The effect of feed concentration on separation efficiency has been studied with the 2 in. diameter column, at a feed rate maintained at 52 $\pm$ 2 cc/min for 3 different feed concentrations: 0.15 g/l, 0.20 g/l, 0.30 g/l. The concentration range was limited by the unstability of the foam at low concentrations and an attempt to keep the bulk concentration below the c.m.c. From Figure 15, it is indicated that the ratios of drain concen-

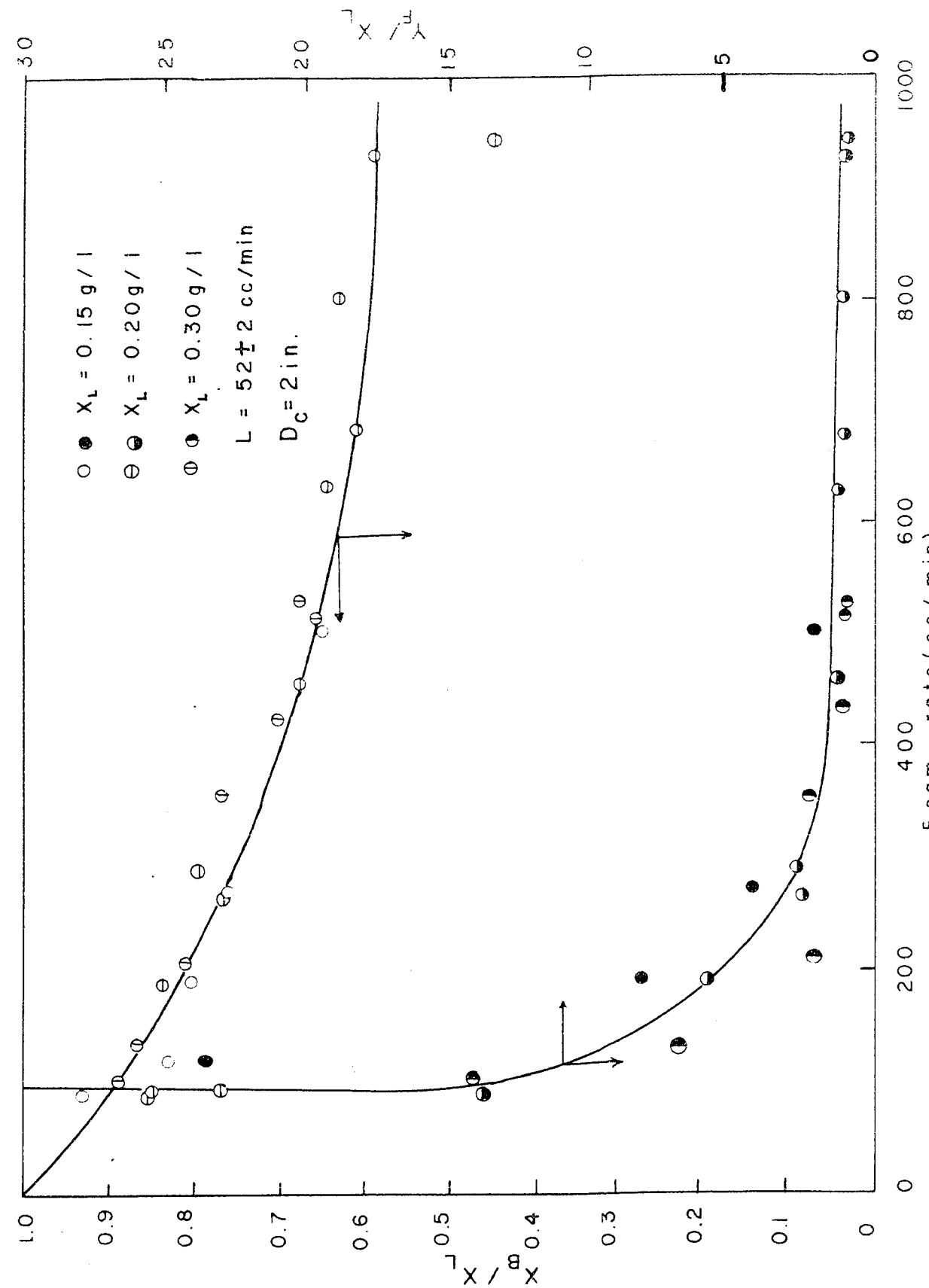

Figure 15. Relationships between separation efficiency and foam rate from variable feed concentration experiments

tration and overhead concentration to feed concentration are independent of feed concentration in the concentration range studied for the 2 in. diameter column at a feed rate of 52 ± 2 cc/min. Since Grieves and Wood (23) have reported that for a given feed concentration, the drain concentration is fixed at a fixed volume of air delivered per unit volume of feed treated it is possible to predict the drain concentration for all feed rates and feed concentrations not exceeding the c.m.c. for a given value of the volume of air delivered per unit volume of feed.

iii. Effect of Foam Height

Since drainage appears to be an important factor in the foam separation process, its effect was studied by keeping the gas rate constant and varying the foam height, thus varying the residence time of the foam bubbles in the column. This was realized by withdrawing the foam from ports of varying heights with respect to the interface.

With the solution-foam interface at 14 in. above the gas sparger a feed concentration of 0.15 g/l and a gas rate of 1600 cc/min (measured at STP), 15 tests were conducted with the 4 in. diameter column by varying the foam height H_F from 2 in. to 50 in. for feed rates L = 24 ± 1 cc/min and 49 ± 1 cc/min.

Fig. 16 shows that for both feed rates, at a short distance above the interface, the collapsed foam (foamate) rate decreased sharply

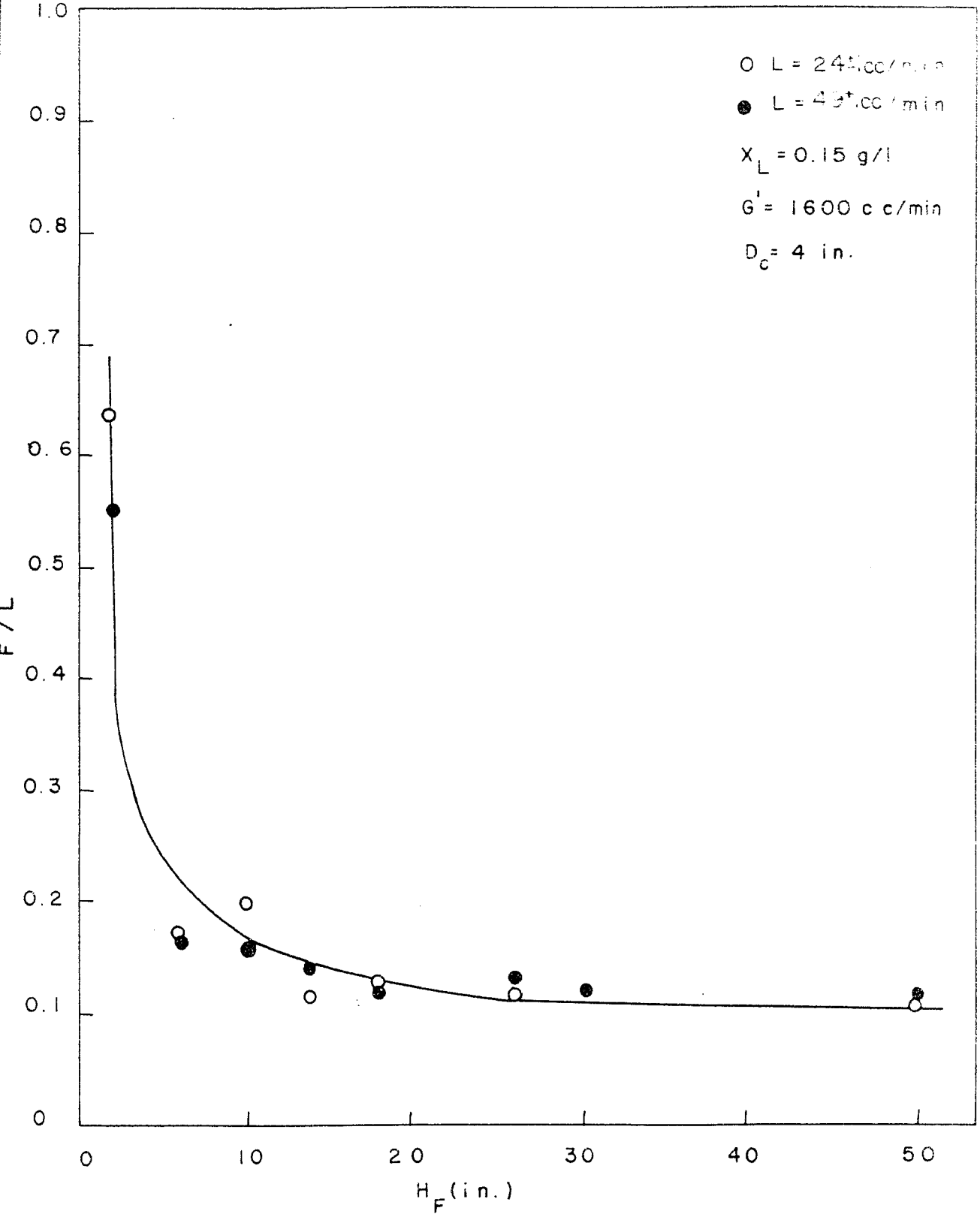

Figure 16. Effect of foam height on foamate rate

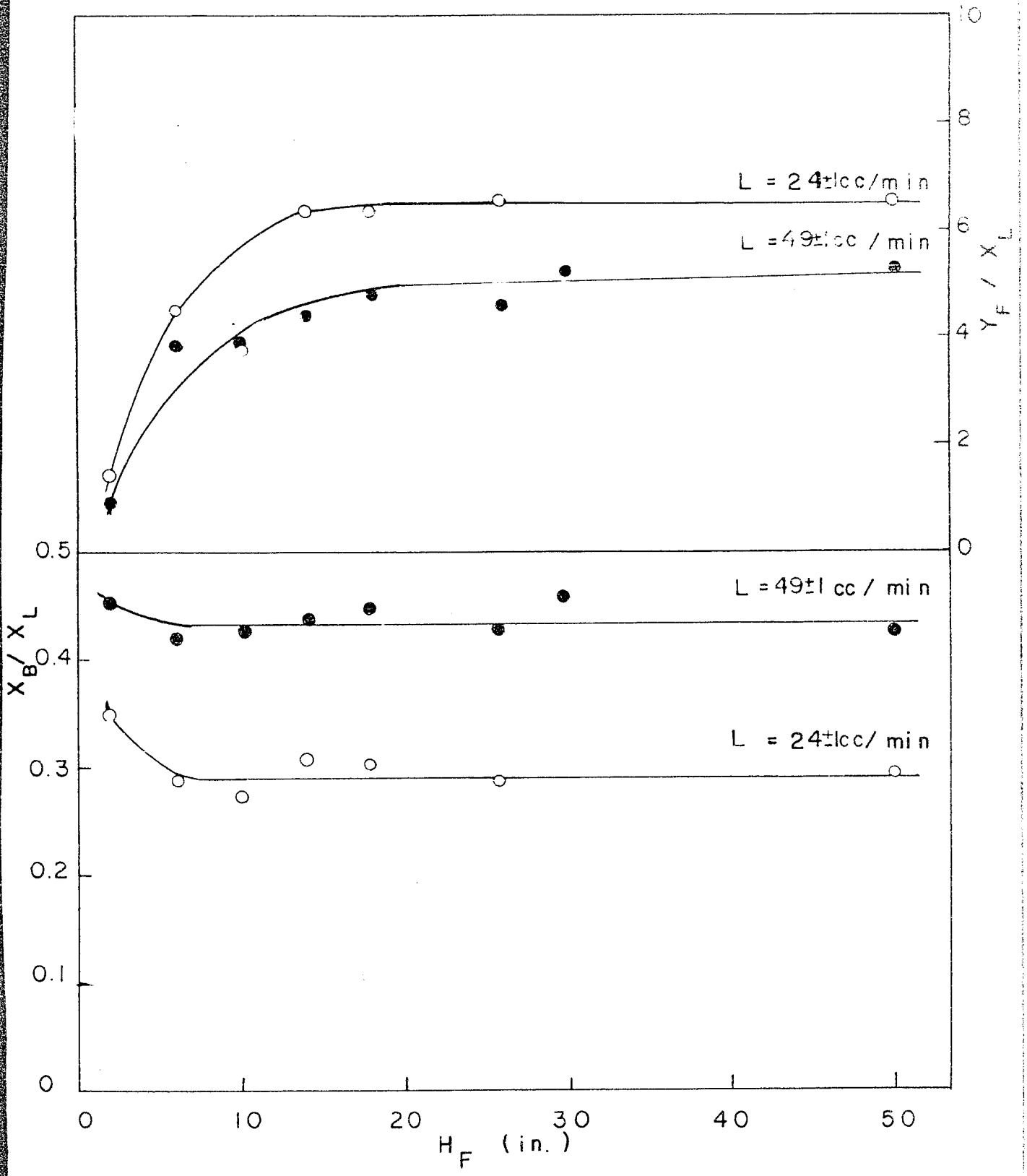

Figure 17. Effect of foam height on drain concentration and foamate concentration

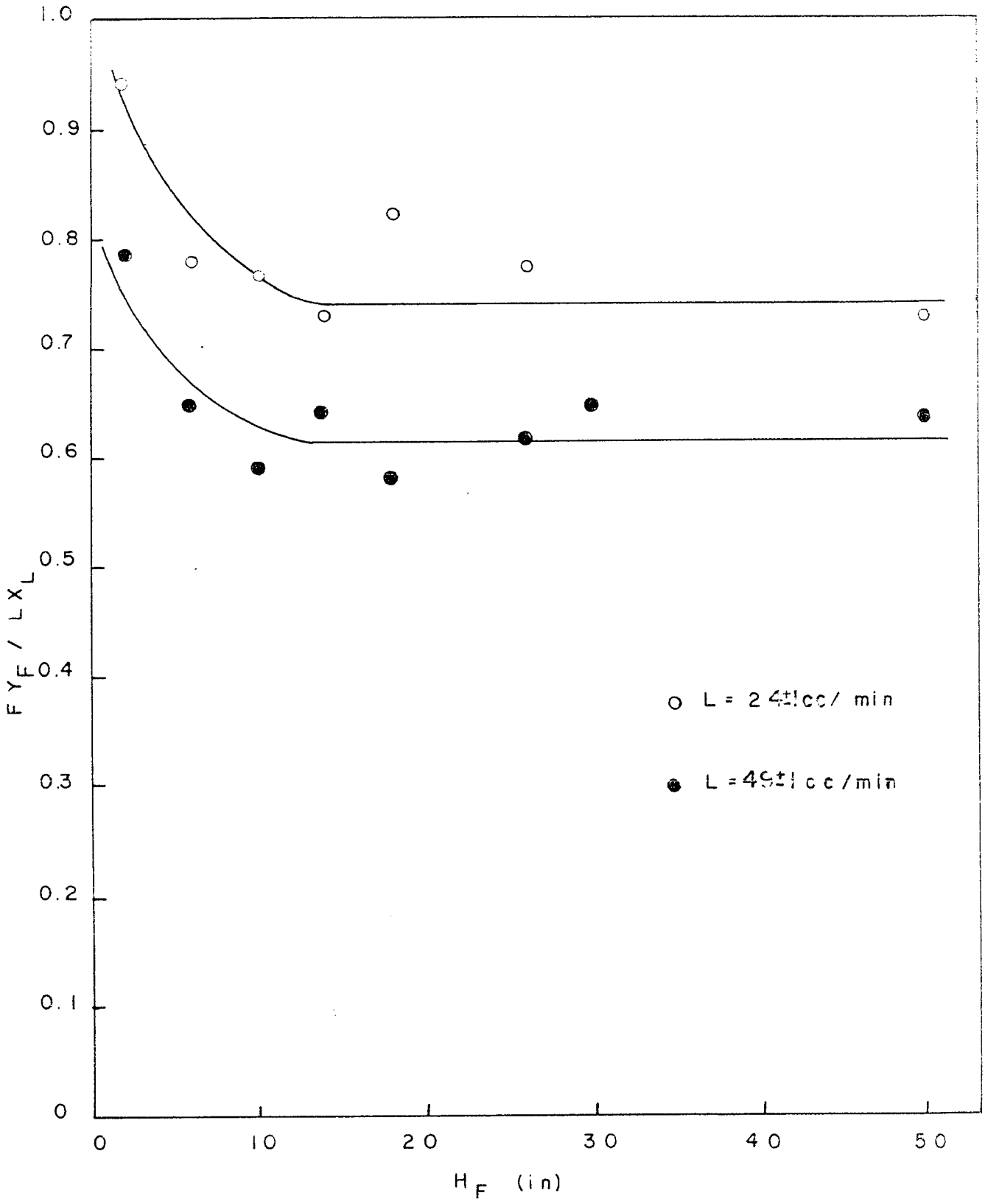

Figure 18. Effect of foam height on removal ratio

due to drainage, then remained almost constant as H_F was further increased. At the same time, for $H_F > 6$ in., x_B was virtually constant, as shown in Fig. 17*. Between $H_F = 6$ in. and $H_F = 18$ in., y_F/x_L increased from 4.55 to 6.43 for $L = 24 \pm 1$ cc/min, and from 3.97 to 4.81 for $L = 49 \pm 1$ cc/min while x_B/x_L remained practically constant. This indicates that a large percentage (although not all) of the entrained liquid was of concentration x_B.

The effect of foam height, and consequently of drainage time on the performance of a foam separation column may be important at low foam heights but becomes negligible if the foam column is high enough to ensure good drainage, provided the foam remains stable.

iv. Effect of Feed Rate

For feed rates of $L = 24 \pm 1$ cc/min and $L = 49 \pm 1$ cc/min, Figures 16 to 18 also show that the ratio F/L was relatively independent of L and that for the same feed concentration ($x_L \simeq 0.15$ g/l), x_B increased and y_F decreased with increasing feed rate. The removal ratio $F y_F / L x_L$, which is a measure of separation efficiency, also increased with decreasing feed rate. This confirmed the observations of Grieves and Wood (22), who

---

* In Fig. 17 x_B/x_L and y_F/x_L were chosen as ordinate instead of x_B and y_F to minimize the effect of minor deviations in x_L, which was in the range 0.150 ± 0.005 g/l.

have concluded that "the liquid residence time of an element of feed in a layer of constant, limited volume, rather than the residence time in the entire column of liquid, is the critical factor affecting the separation". Thus the solution height did not affect the separation efficiency for constant feed rate, gas rate and foam height, while the feed rate did.

v. Effect of Column Diameter

The effect of the diameter of foam separation columns on separation efficiency was studied with 3 different column diameters: 2 in., 4 in. and 6 in. In the three cases, the height of solution above the bubbler was maintained at 14 in. and the height of the foam column above the interface at 53.5 in. The same bubbler (2.5 in. diameter stainless steel porous metal plate, 20 μ pores) was used for the 4 in. and 6 in. columns. For the 2 in. column, the bubbler was cut from the same stainless steel plate and fixed directly to the bottom of the column. For all tests, the feed rate was maintained at 52 $\pm$ 2 cc/min and the feed concentration at 0.15 g/l. The range of gas rates covered was limited by the coalescence of bubbles at very low gas rates and bubble breakage at very high rates.

In Figures 19 to 22, the abscissa is the gas rate G' as measured by the rotameter and the ratios x_B/x_L, y_F/x_L, B/L, F/L have been chosen as ordinates instead of x_B, y_F, B, F in order to minimize the effect of

minor variations in x_L and L which were maintained at $0.015 \pm 0.0005\%$ and 52 ± 2 cc/min respectively. Figures 19 to 22 show that:

(1) The drain rate decreased with increasing gas rate and the rate of decrease of the drain rate became smaller with increasing column diameter. This is due to entrainment which increased the overhead rate. The entrainment effect was more important with smaller columns since the determining factor was the velocity of the gas in the column.

(2) The bottoms concentration decreased with increasing gas rate and levelled off at high gas rates, and for the same gas rate, it was lower as the diameter increased, while the overhead concentration decreased with increasing gas rate and increased with increasing diameter at the same gas rate. At low gas rates, the few bubbles rising caused little stripping. On the other hand, the foam produced rose slowly, draining well and yielding a high enrichment. At very low gas rates, the enrichment was further improved by the internal reflux caused by the breakage of bubbles. This accounted for the very high values of y_F at low gas rates. At high gas rates, the number of bubbles brought into contact with the solution was large. They produced a large interfacial area and strong stripping took place. However, more liquid was entrained with the rapidly rising foam, thus lowering the solute concentration in the overhead and yielding poorer foam.

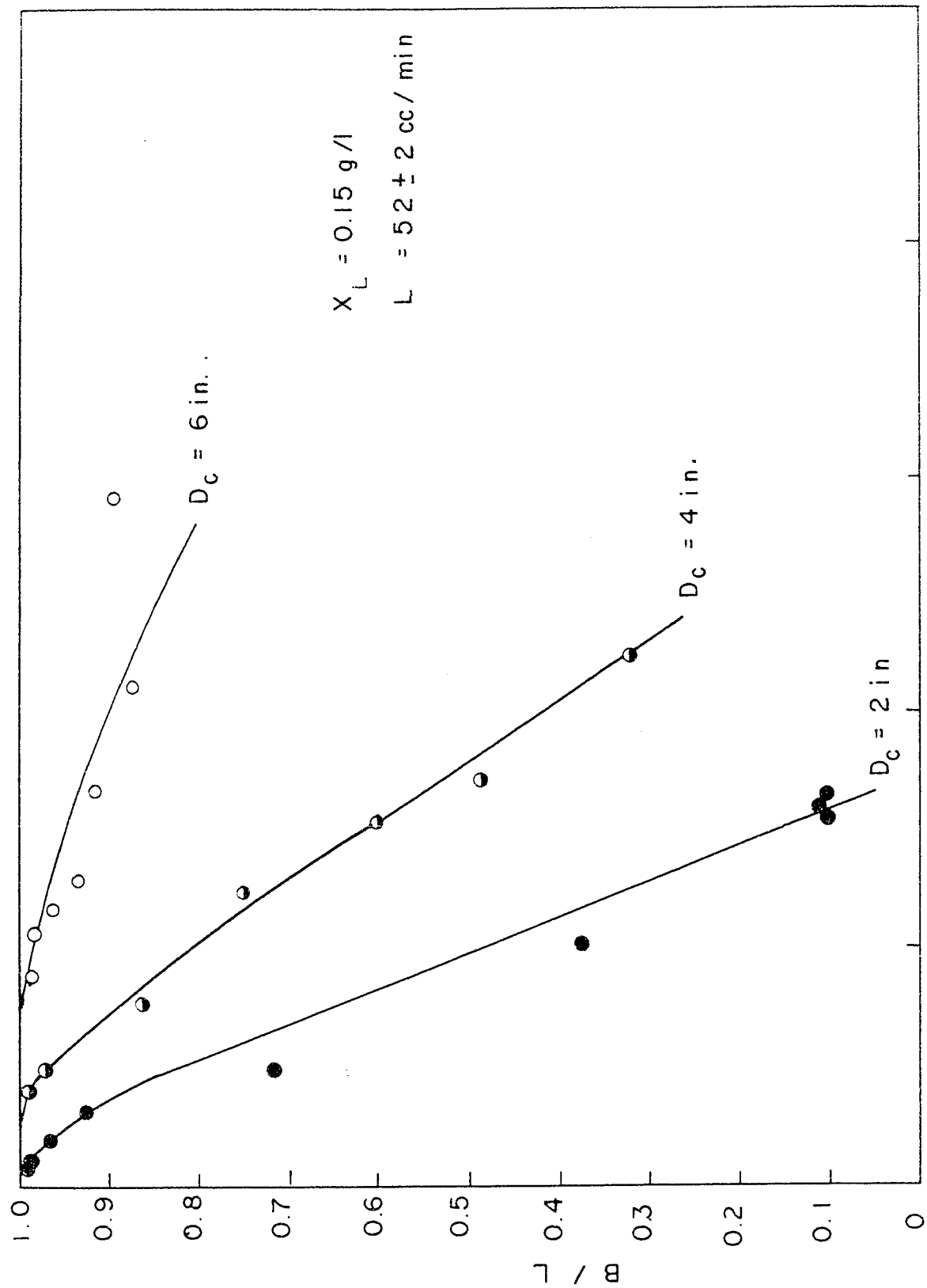

Figure 19. Relationships between B/L and G' from variable column diameter experiments

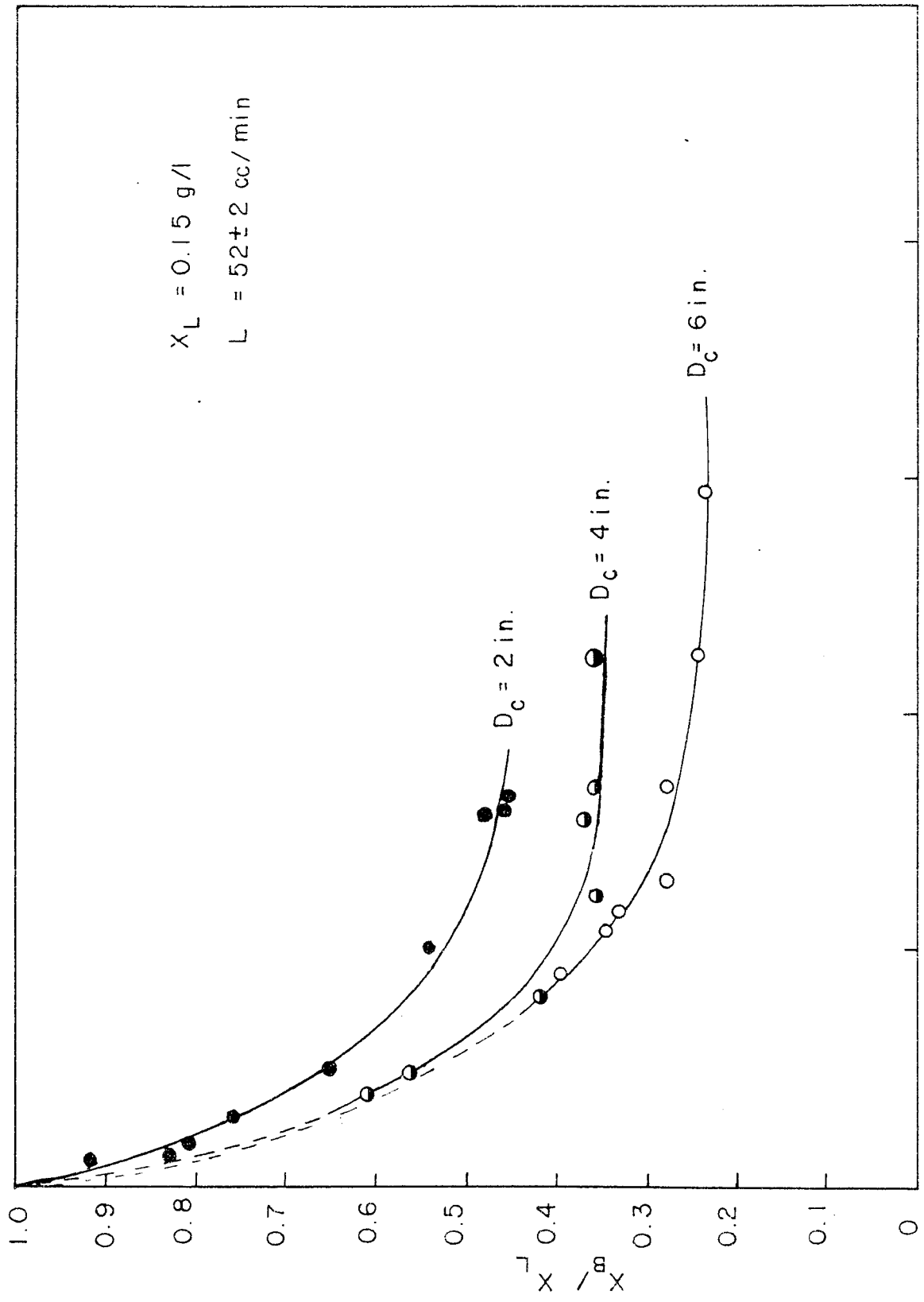

Figure 20. Relationships between X_B / X_L and G' from variable column diameter experiments

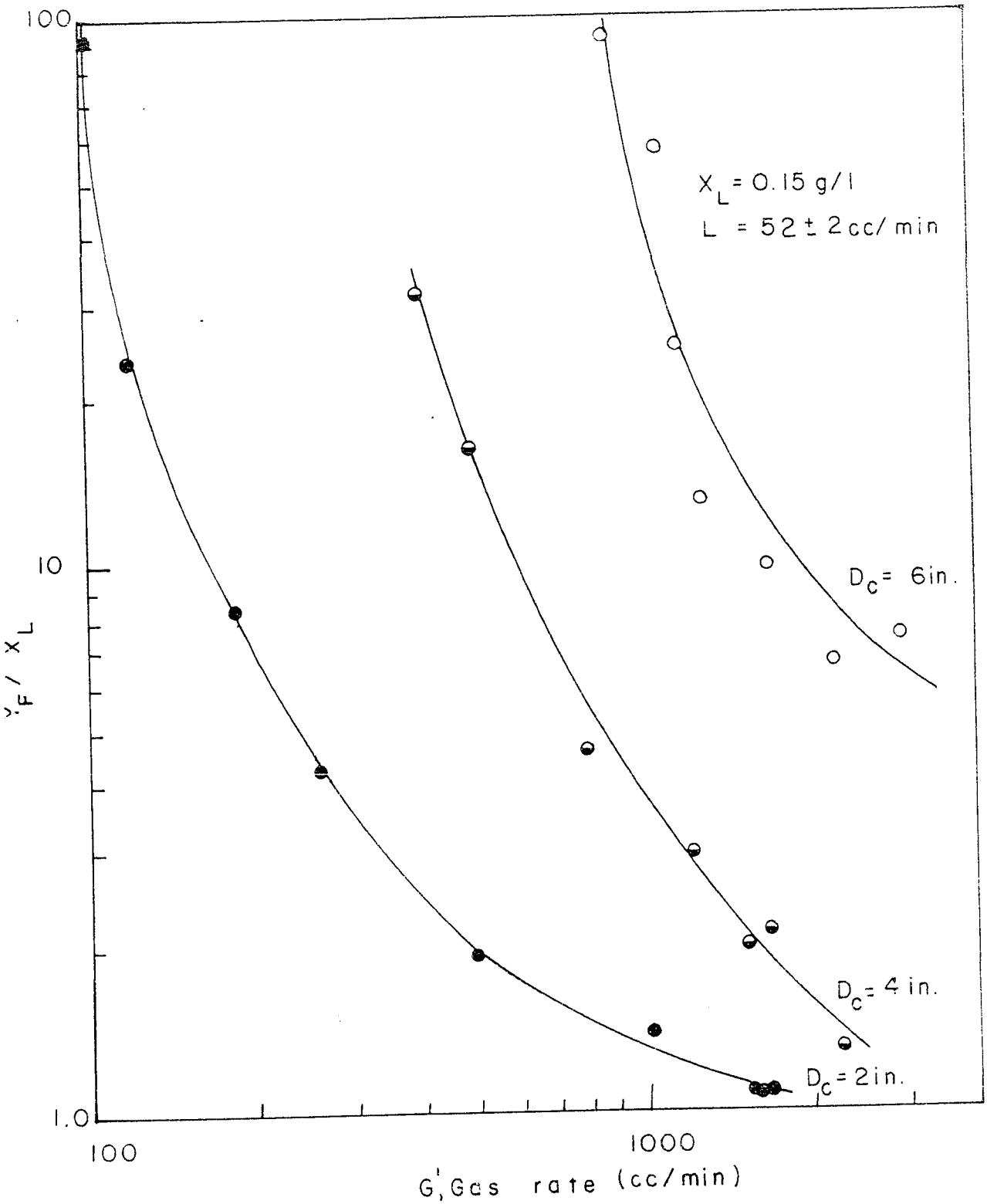

Figure 21. Relationships between Y_F / X_L and G' from variable column diameter experiments

(3) The removal ratio Fy_F/Lx_L increased with increasing gas rate and for the same gas rate, it was higher for the 2 in. column and practically the same for the 4 in. and 6 in. columns.

vi. Conclusion

From the above results, the following observations can be made on the choice of the operating variables in a foam separation process.

The choice of a gas rate to be used will depend on whether it is a stripping or an enriching operation. Since a low value of the ratio x_B/x_L means better stripping, a decontamination operation requires a high gas rate, but operating with a high gas rate necessitates the disposal of a large volume of foam which may be inconvenient. Likewise, an enriching operation would require a low gas rate but the output (i.e., the overhead rate) is also low.

For either objective, it is more advantageous to operate with a large diameter column since at the same gas rate and feed concentration, x_B decreased, and y_F increased markedly with increasing diameter. The use of a large diameter column is particularly advantageous in a stripping operation for better stripping (lower x_B/x_L) and reduced overhead (higher B/L) results. The limiting factor in the choice of the diameter

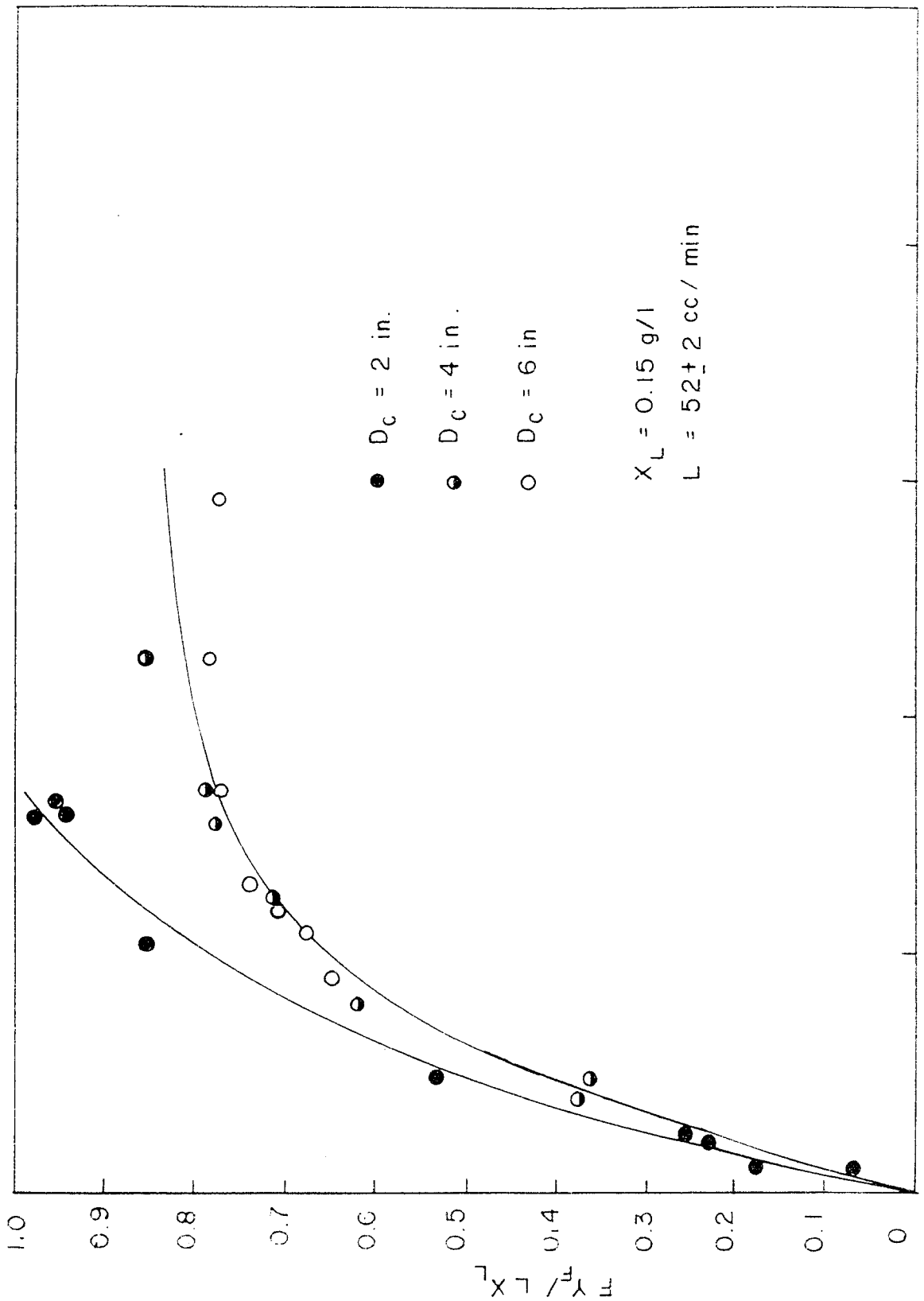

Figure 22. Relationships between removal ratio and gas rate from variable column diameter experiments

of a foam separation column, apart from the equipment cost, is the removal ratio which assesses the overall separation efficiency in terms of the percentage of surfactant removed from the feed stream, and not only in terms of the concentrations of the overhead and drain streams.

VI CONCLUSIONS

Experimental determination of the adsorption of EHDA-Br at liquid-air interface generated by bubbling a constant stream of air through an aqueous solution of that surfactant has shown that the surface excess Γ depends on foam rate as well as bulk solution concentration whereas Gibbs' adsorption isotherm predicts a constant value for Γ. It was therefore concluded that the application of Gibbs' equation to the prediction of the surface excess accumulated at dynamic interfaces generated in the foam separation process for the system EHDA-Br-Water is probably justified only under the rather stringent conditions of good drainage and perfect stability of the foam since coalescence and entrainment seemed to be responsible for the deviations of the experimentally determined surface excess from the theoretical value. Equations proposed to predict the performance characteristics of a continuous pool-feed foam separation column based on Gibbs' equation and an ideal foam model were also found to be valid under the same conditions, provided the interfacial area generated is known with some degree of certainty.

The effects of feed concentration, foam height, feed rate and column diameter on the various parameters describing the separation efficiency of a continuous foam separation column have been studied. It was found that

(1) The ratio of drain concentration and overhead concentration to feed concentration were independent of feed concentration in the concentration range studied, for a feed rate of 52 ± 2 cc/min and a 2 in. diameter column.

(2) The effect of foam height on the performance of a foam separation column, although important at low foam heights, became negligible if the foam column is high enough to ensure good drainage.

(3) The overhead rate was independent of feed rate but the removal ratio increased with decreasing feed rate.

(4) For the same gas rate, feed rate and feed concentration, the performance of a foam separation column improves with increasing column diameter.

A chemical engineering treatment of the foam separation process is possible and a multi-stage separation can be accomplished either by a multi-column scheme or a counter-current foam-feed column (Appendix D).

VII RECOMMENDATIONS FOR FUTURE WORK

An extension of this study to extract traces of metallic ions in an ion flotation process using EHDA-Br as the collector is recommended. It has been reported (21) that cationic surfactants can readily be used for the flotation of chromium and molybdenum in their hexavalent forms (chromate and/or dichromate, molybdate). The effect of operating variables, in particular of pH, surfactant concentration and metal ion concentration should be studied, and a multi-column separation with surfactant recovery could be attempted. The surface excess of the metallic ion as a function of the concentration of the ion in the liquid pool could then be determined with the method used in this study. Finally, a study of the separation efficiency in terms of the HTU's, as outlined in Appendix D could be performed, and perhaps the results could then be employed in an attempt to design a commercially feasible separation process.

REFERENCES

1. Ostwald, W.O., and Siehr, A., Kolloid Z., 76, 33 (1936).

2. Ostwald, W.O., and Mischke, W., Kolloid Z., 90, 17 (1940).

3. Dubrisay, R., Comptes Rendus, 194, 1076 (1932).

4. Schnepf, R.W., and Gaden, E.L. Jr., J. Biochem. Microbiol. Technol. and Eng., 1, 1 (1959).

5. London, M., Cohen, M., and Hudson, P.B., J. Am. Chem. Soc. 75, 1746 (1953).

6. Rubin, E., and Gaden, E.L. Jr., "New Chemical Engineering Separation Techniques", H.M. Schoen, ed., p. 359, Interscience, New York (1962).

7. Boyles, W.A., and Lincoln, R.E., Applied Microbiol. 6, 327 (1958).

8. Eldib, I.A., J. Water Pollution Control Fed. 33, 913 (1961).

9. Kevorkian, V., and Gaden, E.L. Jr., A.I.Ch.E.J. 3, 180 (1957).

10. Rubin, E., Everett, R. Jr., Ind. Eng. Chem. 55, 44 (1963).

11. Brunner, C.A., and Lemlich, R., Ind. Eng. Chem. (Fundamentals) 2, 297 (1963).

12. Harper, D.O., and Lemlich, R., Ind. Eng. Chem. (Process Design and Development), 4, 13 (1965).

13. Kishimoto, H., Kolloid Z., 192, 66 (1963).

14. Grieves, R.B., Crandall, C.J., and Wood, R.K., Int. J. Air Water Pollution 8, 501 (1964).

15. Grieves, R.B., and Wood, R.K., Chemistry in Canada, 15, No. 5, 13 (1963).

16. Rubin, E., Ph.D. Dissertation, Columbia U. (1962).

17. Schonfeld, E., Stanford, R., Mazzella, G., Gosh, D., and Mook, S., Report NYO-9577/1960 (Radiation Applications Inc., New York).

18. Schonfeld, E., Rubin, E., Weinstock, J.J., and Mook, S., Report RAI - 100/1961 (Radiation Applications Inc., New York).

19. Schonfeld, S., Rubin, E., and Everett, R., Report RAI-104/1962 (Radiation Applications Inc., New York).

20. Banfield, D.L., Newson, I.A., and Alder, P.I., Paper presented at A.I.Ch.E. - I. Chem. E. Joint Meeting, London (June 14, 1965).

21. Sebba, F., "Ion Flotation", Elsevier, Amsterdam (1962).

22. Grieves, R.B., and Wood, R.K., Nature, 200, 332 (1963).

23. Idib., A.I.Ch.E.J., 10, 456 (1964).

24. Grieves, R.B., and Battacharyya, D., J. Am. Oil Chem. Soc. 42, 174 (1965).

25. Ibid., Nature, 204, 441 (1964).

26. Ibid., J. Water Pollution Control Fed., 37, 980 (1965).

27. Grieves, R.B. and Wilson, T.E., Nature, 205, 1066 (1965).

28. Grieves, R.B., Wilson, T.E., and Shih, K.Y., A.I.Ch.E.J., 11, 820 (1965).

29. Bikerman, J.J., "Surface Chemistry, Theory and Applications", Academic Press, New York (1958).

30. Adamson, A.W., "Physical Chemistry of Surfaces", Interscience, New York (1960).

31. Langmuir, I., and Schaefer, V. J., J. Am. Chem. Soc. 59, 2400 (1937).

32. Grieves, R.B., Battacharyya, D., Nature, 207, 476 (1965).

33. Berkman, S., and Egloff, G., "Emulsions and Foams", Reinhold, New York (1941).

34. Foulk, C.W., Ind. Eng. Chem., 33, 1086 (1941).

35. Foulk, C.W., and Miller, J.N., Ind. Eng. Chem. 23, 1283 (1931).

36. Hazlehurst, T.W., and Neville, H.A., J. Phys. Chem., 44, 592 (1940).

37. Nakagaki, M., J. Phys. Chem., 61, 1266 (1957).

38. Gibbs, J.W., "Collected Works", Longman Green, New York (1931), Vol. 1, p. 301.

or: "Scientific Papers", Dover, New York (1961), Vol. 1, p. 234.

39. Davies, J.T., and Rideal, E.K., "Interfacial Phenomena", Academic Press, New York (1961).

40. Guggenheim, E.A., and Adam, N.K., Proc. Roy. Soc. (London), A 139, 218 (1943).

41. Brady, A.P., and Brown, A.G., "Monomolecular Layers", H. Sobotka, Ed., p. 33, A.A.A.S., Washington (1954).

42. Cockbain, E.G., and McMullen, A.I., Trans. Faraday Soc. 47, 322 (1951).

43. Kevorkian, V., Ph.D. Thesis, Columbia U. (1958).

44. Lemlich, R., and Brunner, C.A., Ind. Eng. Chem. (Fundamentals) 2, 297 (1963).

45. Langmuir, I., J. Am. Chem. Soc. 39, 1848 (1917).

46. Miles, G.D., Shedlovsky, L., Ross, J., J. Phys. Chem. 49, 93 (1945).

47. Jacobi, W.M., Woodcock, K.E., and Grove, C.S. Jr., Ind. Eng. Chem. 48, 2046 (1956).

48. Haas, P.A., and Johnson, H.F., Paper presented at the ACS National Meeting in Chicago (Aug. 30 - Sept. 4, 1964).

49. Leonard, R.A., and Lemlich, R., A.I.Ch.E.J., 11, 18 (1965).

50. Fanlo, S., Ph.D. Thesis, U. of Cincinnati (1965).

51. Mysels, K.J., Shinoda, K., and Frankel, S., "Soap Films, Studies of their Thinning", Pergamon Press, New York (1959).

52. Wilson, A., Epstein, M.B., and Ross, J., J. Colloid Sci. 12, 345 (1957).

53. McBain, J.W., and Davies, G.P., J. Am. Chem. Soc. 49, 2230 (1927).

54. McBain, J.W., and DuBois, R., J. Am. Chem. Soc. 51, 3534 (1929).

55. McBain, J.W., and Humphreys, C.W., J. Phys. Chem. 36, 301 (1932).

56. Dixon, J.K., Judson, C.M., and Salley, D.J., "Monomolecular Layer", H. Sobotka, ed., American Association for Advancement of Science (1954), p. 63.

57. Eldib, I.A., "Advances in Petroleum Refining", Vol. 7, J.J. McKetta, Ed., Interscience, New York (1963), p. 67.

58. Haas, P.A., and Johnson, H.F., A.I.Ch.E.J., 11, 319 (1965) also: Report ORNL - 3527 (1965).

NOMENCLATURE

a	Interfacial area per unit volume of foam (cm^2/cm^3)
a_i	Activity of the i th component
A	Interfacial area per unit volume of surface layer (cm^2/cm^3)
B	Bottoms (or drain, or raffinate) flow rate (cm^3/min)
D	Effective diameter of bubbles based on surface and volume (cm or mm where indicated)
D_c	Column diameter (in.)
D.F.	Decontamination factor: x_L/x_B
E	Enrichment ratio: y_F/x_B
F	Collapsed foam (foamate) flow rate (cm^3/min)
G	Foam flow rate (cm^3/min)
G'	Gas flow rate (cm^3/min STP)
H_F	Height of foam column above interface (in.)
k_L	Mass transfer coefficient based on the interfacial phase
k_s	Mass transfer coefficient based on the bulk liquid phase
K	A constant representing the decrease in concentration of the bulk liquid (g/cm^3)
l	Foam ratio: F/G (ml liquid/ml foam)
L	Feed flow rate (cm^3/min)
R	Gas constant
s	Cross section of the foam column
S	Surface layer rate (cm^3/min)
S_R	Stripping ratio (x_B/x_L)

T	Absolute temperature (°K)
x_B	Bulk concentration and entrained liquid concentration (g/l or g/cm^3 where indicated)
x_L	Feed concentration (g/l or g/cm^3 where indicated)
y_F	Collapsed foam concentration (g/l or g/cm^3 where indicated)
y_s	Surface layer concentration (g/l or g/cm^3 where indicated)
Z	Height of foam column as determined from equations (35) and (36)
γ	Surface tension (dynes/cm)
Γ	Surface excess (g/cm^2)
μ_i	Thermodynamic "chemical potential" of the i th component

APPENDIX A

TABULATION OF DATA

Table 5

Single-Stage Equilibrium Studies

Column diameter: 2 in.

Batch operation with total recirculation

x_B (g/l)	G cm^3/min	y_F (g/l)	D (cm)	E	1	Γ_{exp} (g/cm^2) x 10^8
0.146	230.4	1.047	0.079	7.16	0.0052	6.20
0.151	237.0	1.020	0.105	6.78	0.0054	8.14
0.149	282.0	0.585	0.076	3.94	0.0126	6.94
0.145	373.8	0.407	0.090	2.81	0.0185	7.28
0.152	525.6	0.340	0.095	2.24	0.0205	6.15
0.147	681.0	0.300	0.109	2.04	0.0257	7.10
0.153	937.8	0.236	0.133	1.84	0.0300	8.49

Table 5 (Continued)

x_B (g/l)	G cm^3/min	y_F (g/l)	D (cm)	E	l	$(g/cm^2)^{exp} \times 10^8$
0.199	83.4	1.567	0.095	78.83	0.0005	12.75
0.181	240.6	0.854	0.092	4.71	0.0095	9.28
0.197	325.2	0.675	0.078	3.43	0.0166	8.00
0.191	486.6	0.488	0.077	2.56	0.0190	7.25
0.200	748.2	0.423	0.094	2.12	0.0265	9.28
0.299	138.6	4.246	0.089	14.20	0.0024	13.90
0.307	204.0	1.240	0.071	3.35	0.0149	12.75
0.298	252.6	0.993	0.094	3.33	0.0100	10.89
0.297	253.2	1.094	0.094	3.68	0.0090	11.23
0.294	521.4	0.592	0.092	2.01	0.0180	9.83
0.319	593.4	0.205	0.095	2.05	0.0180	10.03

Table 6

Continuous Foam Separation: Validity of the ideal foam model

Effect of feed concentration on separation efficiency

Column diameter: 2 in.

x_L (g/l)	G (cm^3/min)	L (cm^3/min)	F (cm^3/min)	B (cm^3/min)	D (cm)	x_B (g/l)	y_F (g/l)	y_F/x_L	x_B/x_L
0.150	91.4	52.4	0.04	52.4	0.122	0.140	14.300	95.30	0.93
0.151	121.6	51.9	0.4	51.5	0.103	0.125	3.360	23.80	0.83
0.151	192.0	52.5	1.5	51.0	0.089	0.122	1.230	8.15	0.81
0.149	271.4	52.75	3.25	49.5	0.083	0.114	0.634	4.24	0.76
0.150	503.2	50.5	14.0	36.5	0.086	0.098	0.291	1.94	0.65
0.202	93.5	50.3	0.35	50.0	0.112	0.178	4.667	23.10	0.83
0.200	187.1	52.8	1.3	51.5	0.080	0.168	1.135	5.67	0.84
0.202	265.1	50.5	6.5	44.0	0.066	0.155	0.483	2.39	0.77
0.203	289.4	50.1	5.1	45.0	0.078	0.162	0.564	2.77	0.80
0.202	453.6	50.0	24.5	25.5	0.066	0.139	0.251	1.24	0.69
0.202	629.9	51.3	25.0	26.3	0.071	0.130	0.248	1.23	0.64
0.202	683.1	53.5	36.0	17.5	0.068	0.124	0.241	1.19	0.61
0.200	800.8	49.5	29.0	20.5	0.088	0.127	0.237	1.18	0.63
0.202	942.0	50.0	50.0	0.0	0.090	0.090	0.202	1.02	0.59

Table 6 (Continued)

x_L (g/l)	G (cm^3/min)	L (cm^3/min)	F (cm^3/min)	B (cm^3/min)	D (cm)	x_B (g/l)	y_F (g/l)	y_F/x_L	x_B/x_L
0.303	130.7	51.5	1.0	50.5	0.066	0.265	2.018	6.67	0.87
0.301	207.5	50.0	7.5	42.5	0.050	0.246	0.617	2.05	0.81
0.303	356.0	53.0	20.5	32.5	0.047	0.229	0.382	1.27	0.77
0.301	435.8	48.5	32.5	16.0	0.044	0.212	0.345	1.14	0.70
0.302	514.0	50.5	45.5	5.0	0.047	0.202	0.316	1.04	0.66
0.301	529.0	50.0	45.0	5.0	0.056	0.205	0.310	1.03	0.68

Table 7

Continuous Foam Separation: Effect of foam height and feed rate on separation efficiency

Column diameter: 6 in.

Gas rate: G' = 1600 cc/min

H_F (in)	x_L (g/l)	L cc/min	F cc/min	x_B (g/l)	y_F (g/l)	F/L	x_B/x_L	y_F/x_L	Fy_F/Lx_L
2	0.151	25.0	15.0	0.053	0.217	0.64	0.35	1.43	0.95
6	0.152	25.3	4.4	0.044	0.690	0.17	0.29	4.55	0.78
10	0.151	23.8	4.8	0.041	0.575	0.20	0.27	3.81	0.77
14	0.149	23.4	2.8	0.046	0.951	0.12	0.31	6.39	0.73
18	0.149	24.8	3.2	0.045	0.957	0.13	0.30	6.43	0.83
26	0.149	25.0	3.0	0.043	0.976	0.12	0.29	6.58	0.77
50	0.150	25.1	2.8	0.044	0.986	0.11	0.29	6.59	0.74
2	0.153	49.3	27.2	0.070	0.219	0.55	0.46	1.43	0.79
6	0.152	49.7	8.1	0.064	0.605	0.16	0.42	3.97	0.65
10	0.151	48.8	7.7	0.065	0.580	0.16	0.43	3.85	0.59
14	0.148	49.5	7.2	0.065	0.654	0.14	0.44	4.41	0.64
18	0.146	48.5	5.9	0.066	0.704	0.12	0.45	4.81	0.58
26	0.149	49.0	6.5	0.064	0.696	0.13	0.43	4.65	0.62
30	0.149	49.0	6.0	0.069	0.791	0.12	0.46	5.30	0.65
50	0.148	50.4	6.1	0.063	0.776	0.12	0.43	5.26	0.64

Table 8a

Continuous Foam Separation: Effect of column diameter on separation efficiency

Column diameter: 2 in.

Foam column height: H_F = 53.5 in.

x_L (g/l)	G (cc/min)	L (cc/min)	B (cc/min)	B/L	x_B (g/l)	y_F (g/l)	x_B/x_L	y_F/x_L	$F y_F/L x_L$
0.150	100	52.4	52.4	1.000	0.140	14.300	0.93	95.30	0.067
0.151	120	51.9	51.5	0.994	0.125	3.600	0.83	23.80	0.179
0.151	185	52.5	51.0	0.972	0.122	1.230	0.81	8.15	0.234
0.150	260	52.75	49.5	0.938	0.114	0.634	0.76	4.24	0.261
0.151	500	50.5	36.5	0.723	0.098	0.291	0.65	1.94	0.538
0.150	1020	52.0	20.0	0.385	0.082	0.212	0.54	1.40	0.864
0.150	1570	50.7	5.2	0.103	0.072	0.164	0.48	1.09	0.983
0.150	1600	54.0	6.0	0.111	0.069	0.159	0.46	1.06	0.942
0.150	1668	53.45	6.75	0.104	0.068	0.164	0.45	1.09	0.955

Table 8b

Continuous Foam Separation: Effect of column diameter on separation efficiency

Column diameter: 4 in.

Foam column height: H_F = 53.5 in.

x_L (g/l)	G' (cc/min)	L (cc/min)	B (cc/min)	B/L	x_B (g/l)	y_F (g/l)	x_B/x_L	x_B/x_L	$F y_F/L x_L$
0.150	400	50.6	50.0	0.988	0.091	4.708	0.61	31.39	0.384
0.151	500	52.7	51.5	0.975	0.085	2.456	0.56	16.27	0.371
0.150	800	51.0	44.0	0.864	0.063	0.687	0.42	4.58	0.624
0.151	1225	55.6	42.0	0.756	0.055	0.450	0.36	2.98	0.729
0.150	1550	52.0	31.5	0.605	0.056	0.298	0.37	1.99	0.783
0.151	1700	53.5	24.5	0.490	0.054	0.337	0.36	2.25	0.793
0.150	2250	50.0	16.0	0.320	0.054	0.190	0.36	1.27	0.861

Table 8c

Continuous Foam Separation: Effect of column diameter on separation efficiency

Column diameter: 6 in.

Foam column height: H_F = 53.5 in.

x_L (g/l)	G' (cc/min)	L cc/min	B cc/min	B/L	x_B (g/l)	y_F (g/l)	x_B/x_L	y_F/x_L	Fy_F/Lx_L
0.151	900	50.4	50.0	0.99	0.061	0.137	0.40	91.11	0.650
0.151	1100	51.1	50.5	0.99	0.052	0.087	0.35	57.69	0.677
0.151	1175	52.5	51.0	0.97	0.050	0.038	0.33	24.99	0.715
0.151	1300	53.5	50.5	0.94	0.043	0.020	0.28	13.17	0.738
0.151	1700	52.1	48.0	0.92	0.043	0.015	0.28	9.88	0.777
0.151	2240	53.3	46.8	0.88	0.039	0.010	0.25	6.59	0.788
0.151	2930	53.7	48.3	0.90	0.036	0.012	0.24	7.35	0.776

APPENDIX B

POTENTIOMETRIC ANALYSIS OF EHDA-Br

POTENTIOMETRIC ANALYSIS OF EHDA-Br

Instruments

The instruments used for the analysis of EHDA-Br were a Beckman (No. H2) pH meter, a silver billet electrode (Beckman Catalog No. 39261), a sealed calomel reference electrode (Beckman Catalog No. 39970) and a magnetic stirrer.

Reagent

A stock solution of $AgNO_3$ was prepared by dissolving approximately 2.40 g of $AgNO_3$ in a 1-liter volumetric flask. The solution was standardized against a standard 0.014N KCl solution. The $AgNO_3$ stock solution was diluted twenty times to give a solution of approximately 0.0007 N.

Titration Procedure

25 ml of the feed solution, 50 ml of the bottoms sample, and 50 ml of a foam sample diluted 10 times were analyzed each time. The e.m.f. was recorded after every addition of $AgNO_3$ titrant and a plot of e.m.f. versus volume of titrant added was used to determine the end point.

Accuracy: 0.2 ml $AgNO_3$ ($\pm$ 0.002 g/l EHDA-Br).

APPENDIX C

SAMPLE CALCULATIONS

SAMPLE CALCULATIONS

I. Surface excess from surface tension data

From equation (5)

$$\Gamma = -\frac{1}{2RT}\frac{d\gamma}{d\ln x_B}$$

where $\frac{d\gamma}{d\ln x_B}$ = slope of Figure 5

= - 11.32 dynes/cm

For T = 23° C = 296° K

$$\Gamma = \frac{1 \times 11.32}{2 \times (8.314 \times 10^7) \times 296} = 2.30 \times 10^{-10} \text{ g-moles/cm}^2$$

$$= 2.30 \times 10^{-10} \times 378.5 \frac{\text{g}}{\text{g-mole}} = 8.70 \times 10^{-8} \text{ g/cm}^2$$

For T = 28° C = 301° K

$$\Gamma = 2.26 \times 10^{-10} \text{ g-moles/cm}^2 = 8.56 \times 10^{-8} \text{ g/cm}^2$$

Average: $\Gamma = 2.28 \times 10^{-10}$ g-moles/cm^2 = 8.63×10^{-8} g/cm^2

II. Molecular Area

Assuming adsorption in a monomolecular layer:

$$\text{Molecular area} = \frac{1}{2.28 \times 10^{-10}} \frac{\text{cm}^2}{\text{g-mole}} \times \frac{1}{6.024 \times 10^{23}} \frac{\text{g-mole}}{\text{molecules}}$$

$$\times \frac{1 \times 10^{-4} \text{ m}^2}{\text{cm}^2} \times \frac{1 \text{ A}^{\circ 2}}{1 \times 10^{-20} \text{ m}^2} = 72.8 \text{ A}^{\circ 2}$$

III. Surface excess from foam separation with recycling data

From equation (15)

$$\Gamma = (E - 1) \frac{D1\, x_B}{6}$$

Example: Table 5, First run

$$y_F = 1.047\ g/l = 1.047 \times 10^{-3}\ g/cm^3$$

$$x_B = 0.146\ g/l = 0.146 \times 10^{-3}\ g/cm^3$$

$$E = \frac{y_F}{x_B} = \frac{1.047}{1.046} = 7.16$$

$$D = 0.079\ cm$$

$$\Gamma = (7.16 - 1) \frac{0.079\ (cm) \times 0.146 \times 10^{-3}\ (g/cm^3)}{6}$$

$$= 6.20 \times 10^{-8}\ g/cm^2$$

IV. Surface excess from continuous foam separation data

From equations (23) and (24)

$$\Gamma_B = (\frac{x_L}{x_B} - 1)\ (\frac{L}{G}\ \frac{D}{6})\ x_B$$

$$\Gamma_F = (\frac{y_F}{x_B} - 1)\ (\frac{F}{G}\ \frac{D}{6})\ x_B$$

Example: Table 6, First run

$$x_L = 0.150\ g/l = 0.150 \times 10^{-3}\ g/cm^3$$

$$x_B = 0.140\ g/l = 0.140 \times 10^{-3}\ g/cm^3$$

$$y_F = 14.300\ g/l = 14.300 \times 10^{-3}\ g/cm^3$$

$L = 52.4\ cm^3/min$

$G = 91.4\ cm^3/min$

$F = 0.04\ cm^3/min$

$B = 52.4\ cm^3/min$

$D = 0.122\ cm$

$$\Gamma_B = \left(\frac{0.150}{0.140} - 1\right)\left(\frac{52.4}{91.4} \times \frac{0.122}{6}\right) \times 0.140 \times 10^{-3}$$

$$= 11.65 \times 10^{-8}\ g/cm^2$$

$$\Gamma_F = \left(\frac{14.300}{0.140} - 1\right)\left(\frac{0.04}{91.4} \times \frac{0.122}{6}\right) \times 0.140 \times 10^{-3}$$

$$= 12.55 \times 10^{-8}\ g/cm^2$$

V. Verification of equations (20 - 22)

$$(y_F - x_B)\,FD = (14.300 - 0.140) \times 10^{-3} \times 0.04 \times 0.122$$

$$= 0.690 \times 10^{-4}\ (g - cm)/min$$

$$(x_L - x_B)\,LD = (0.150 - 0.140) \times 10^{-3} \times 52.4 \times 0.122$$

$$= 0.639 \times 10^{-4}\ (g - cm)/min$$

$$(y_F - x_B)\frac{LFD}{B} = (14.300 - 0.14) \times 10^{-3} \times \frac{52.4 \times 0.04 \times 0.122}{52.4}$$

$$= 0.675 \times 10^{-4}\ (g - cm)/min$$

Slope of the theoretical curve (Figure 12)

$$-\frac{3}{RT}\frac{d\gamma}{d\ln x_B} = \frac{3 \times 378.5\ \left(\frac{g}{g - mole}\right) \times 11.32\ \left(\frac{dynes}{cm}\right)}{8.314 \times 10^7\ \left(\frac{dynes - cm}{^\circ K\ g\text{-}mole}\right) \times 298^\circ K} = 5.18 \times 10^{-7}\ g/cm^2$$

APPENDIX D

DESIGN CONSIDERATIONS

DESIGN CONSIDERATIONS

1. The Pool-feed System

In the absence of internal reflux and provided the liquid pool is well mixed, the foam separation column where the feed is admitted into the liquid phase, may be considered as a single equilibrium stage under "ideal" conditions.

For each stage, the Decontamination Factor is:

$$D.F. = \frac{x_L}{x_B} = 1 + \left(\frac{\Gamma}{x_B}\right) \frac{6G}{LD} \qquad (27)$$

with the usual assumptions that the bubbles are spherical and the liquid entrained by the foam is of concentration x_B.

The D. F. depends on the surfactant (Γ/x_B) and the ratio of surface area generated to the feed flow rate (6G/LD). It is constant from stage to stage under the same conditions of surface area generation if the distribution factor Γ/x_B is constant. This is the case for many surfactants and particularly for metal ions (20), although it is not so for EHDA-Br.

The overall D. F. can therefore be greatly improved in a multi-column scheme where the raffinate (drain) solution from each column is fed to the next. In the simplest case where the surface area generated per unit feed flow rate and Γ/x_B are constant the overall decontamination factor for n columns would be:

$$(D.F.)_{n\ \text{columns}} = (D.F.)^{n}_{\text{single column}} \qquad (28)$$

In the case of EHDA-Br, Γ is constant in the region where Gibbs' equation can be applied. For the multi-column system represented by Figure 23, where the drain product of a column is fed into the next column and where the foam is withdrawn separately from the top of each column, the concentration of the raffinate from each column is related to the concentration of the feed to the column by the following equation:

$$x_n = x_{n+1} + \Gamma \frac{6G}{DL}$$

If the ratio of the interfacial area generated to the feed flow rate is maintained constant (by maintaining the same ratio of gas rate to feed rate for each column and provided the diameter of the bubbles does not vary too much), it can be written:

$$x_n = x_{n+1} + K \qquad (29)$$

where $K = \Gamma \frac{6G}{DL}$ represents the decrease in concentration due to enrichment of the interfacial phase.

For the (n + 1) stage:

$$(D.F.)_{n+1} = \frac{x_n}{x_{n+1}} = 1 + \frac{\Gamma}{x_{n+1}} \frac{6G}{LD} = 1 + \frac{K}{x_{n+1}}$$

$$\frac{x_n}{x_n + 1} = 1 + \frac{K}{x_n - K}$$

And

$$\frac{x_n}{x_{n+2}} = \frac{x_n}{x_{n+1}} \times \frac{x_{n+1}}{x_{n+2}} = \left(1 + \frac{K}{x_n - K}\right)\left(1 + \frac{K}{x_n - 2K}\right)$$

Since:

$$x_{n+2} = x_{n+1} - K = x_n - 2K$$

The overall D. F. for the N stages of the system represented by Figure 23 is:

$$\text{D. F.} = \frac{x_o}{x_N} = \left(1 + \frac{K}{x_o - K}\right)\left(1 + \frac{K}{x_o - 2K}\right) \cdots\cdots \left(1 + \frac{K}{x_o - NK}\right)$$

$$\text{D. F.} = \frac{x_o}{x_N} = \prod_{n=1}^{n=N} \left(1 + \frac{K}{x_o - nK}\right) \qquad (30)$$

For the simple case discussed above, the number of theoretical stages required to bring a solution of concentration x_o to a raffinate of concentration x_N can be easily predicted graphically. In Figure 24, the "equilibrium line" which relates the feed concentration to the raffinate concentration for each column, it follows that for a surfactant with a constant surface excess such as EHDA-Br, and under the conditions of the case discussed above, the "equilibrium line" is parallel to the diagonal since x_L differs from x_B by only a constant (equation 29). Since the feed

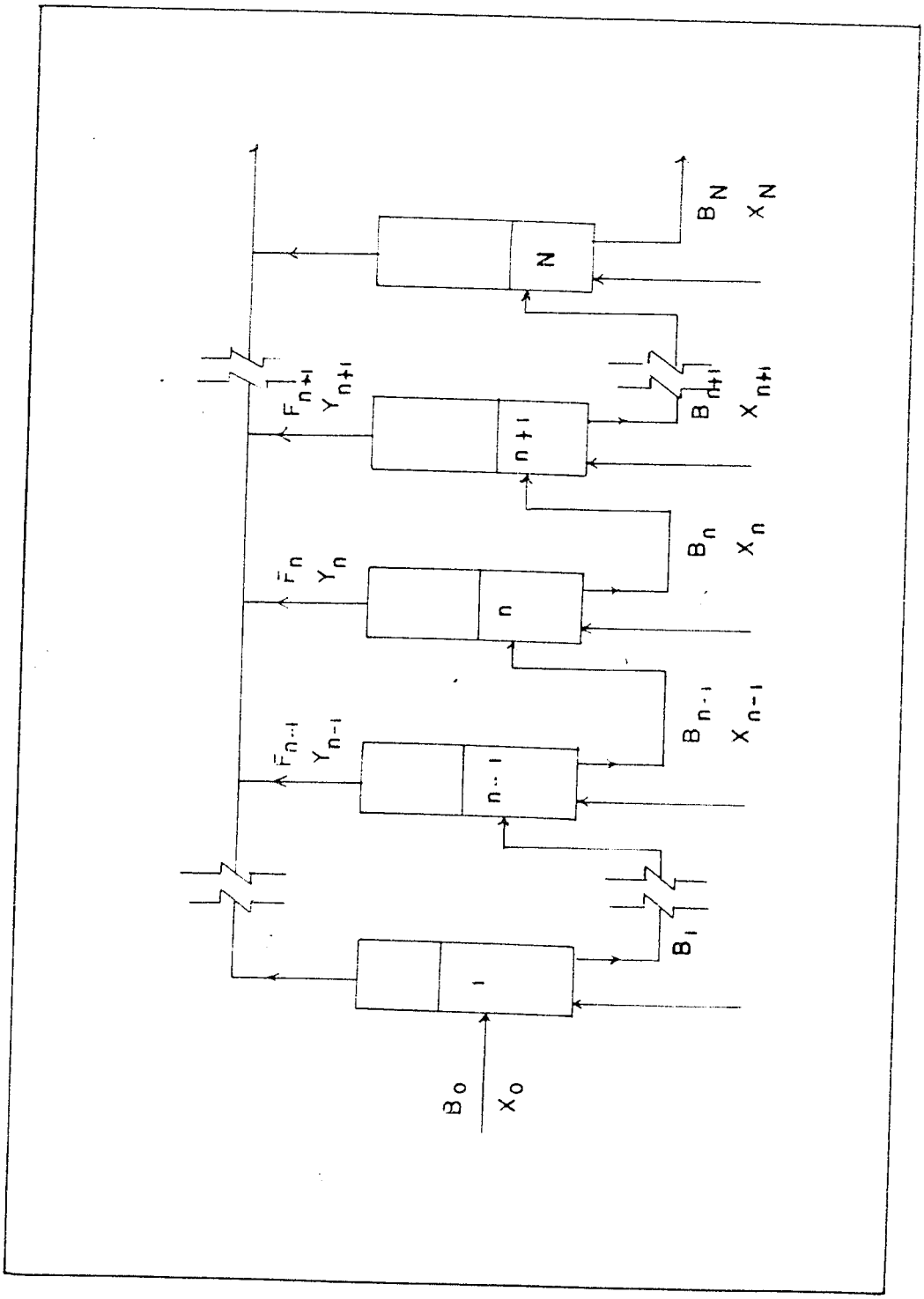

Figure 23. Multi-column pool-feed scheme

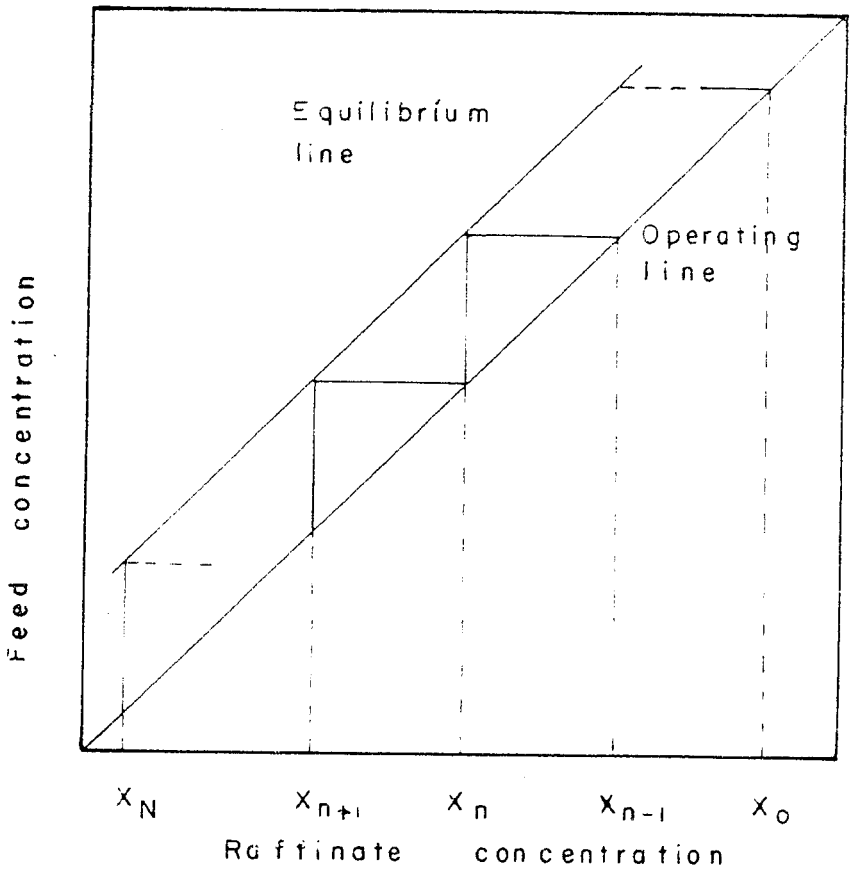

Figure 24. Graphical determination of number of theoretical stages

for a column is the raffinate of the previous column, the "operating line" coincides with the diagonal and it can be seen from Figure 25 that the number of theoretical stages required for a given overall D.F. is seen to decrease if the "equilibrium" line lies farther from the operating line. This can be obtained by using a larger ratio of air rate to feed rate for each column but the foam output will also increase.

2. The Foam-feed System: Analogy with Distillation

To achieve a multi-stage operation, an alternative to the use of multi-column schemes is to introduce the feed into the foam phase, with reflux of the collapsed foam at the top of the foam column. Such an arrangement could provide contact of the gas phase with liquid of increasing concentration along the foam column, thus achieving a multi-stage enriching operation with a single column. Although foam separation is in principle a separation process taking advantage of a natural composition difference within a single phase, it presents a striking resemblance to many two-phase separation processes, in particular to distillation. A qualitative comparison between distillation and foam separation has been made by Rubin and Gaden (6). The main features of the analogy are:

(1) Analogy between the liquid phase in distillation and the bulk liquid in foam separation.

(2) Analogy between the vapor phase in distillation and the foam in foam separation.

(3) Analogy between the heat input in distillation to the gas-liquid interfacial area generated per unit time in foam separation.

Furthermore, features like entrainment (caused by excessive heat or gas input), internal reflux (caused by condensation or foam breakage), are common to both distillation and foam separation. The main difference between distillation and foam separation lies in the fact that in foam separation surface phenomena are involved. For example, in foam separation there is no definite "equilibrium curve" relating the concentration of the foam phase to that of the liquid phase since Gibbs' equation, which is the only quantitative relationship available, predicts an enrichment at the surface layer in terms of surface area rather than volume and a relation between surface area and foam volume must therefore be known.

Despite those difficulties, an attempt has been made by Eldib (57) to adapt the McCabe-Thiele diagram method to determine the number of ideal stages in a foam separation column. However, the validity of this rather unsophisticated approach is somewhat doubtful, since Eldib's analysis is based on several unrealistic assumptions. In particular, a constant foam/liquid mole ratio all through the column was assumed, by analogy with the approximation of constant molal overflow involved in

distillation. The effect of internal reflux was neglected, and the method requires the knowledge of the interfacial area generated.

3. The Counter-current Foam Separation Column

When the feed is introduced into the liquid pool, the system formed by the liquid pool and the foam column represents a single equilibrium stage. The interfacial phase carried by the foam is in equilibrium with the relatively dilute liquid in the liquid pool and any improvement on the overall concentration of the collapsed foam obtained by increasing the height of the foam column is due exclusively to drainage, in the absence of reflux. However, the effect of drainage is limited, as seen in Figure 17. In the absence of reflux, the most efficient operation occurs when the feed is introduced at the top of the column. In such an arragement, the interfacial phase carried by the foam is in contact with liquid of increasing concentration as it moves up along the column. The enrichment of the foam phase will then be due to mass transfer between the "bulk" liquid phase and the interfacial phase in addition to drainage.

The system formed by a foam column with feeding at the top can be treated as a countercurrent mass transfer process analogous to classical separation techniques such as absorption, humidification, etc.

4. The Concept of HTU Applied to Countercurrent Foam Columns*

Fig. 25 is a schematic diagram of a countercurrent foam column. x_o, y_o and x_1, y_1 are the compositions of the bulk liquid and the interfacial layer streams at the feed point and at the bottom of the foam column respectively. It is assumed that the feed is evenly distributed for efficient countercurrent contact throughout the whole column. For steady-state operating conditions, the material balances written for the differential element dz are

Total material balance $$dL = dS \tag{31}$$

Component balance $$d(Lx) = d(Sy) \tag{32}$$

where L = Bulk liquid flow rate (g/hr)

S = Interfacial layer flow rate (g/hr)

x = Concentration of bulk liquid (weight fraction)

y = Concentration of interfacial layer (weight fraction)

Entrained liquid is not taken into account in equations (31) and (32). Since the surfactant concentrations in both phases are very low and assuming that the interfacial flow rate is constant through the column (i.e. neglecting the entrainment), integration of equation (32) from the bottom of the foam column to any height z, yields

$$L(x - x_1) = S(y - y_1) \tag{33}$$

---

* In this section exclusively, flow rates and concentrations are expressed in g/hr and weight fraction respectively.

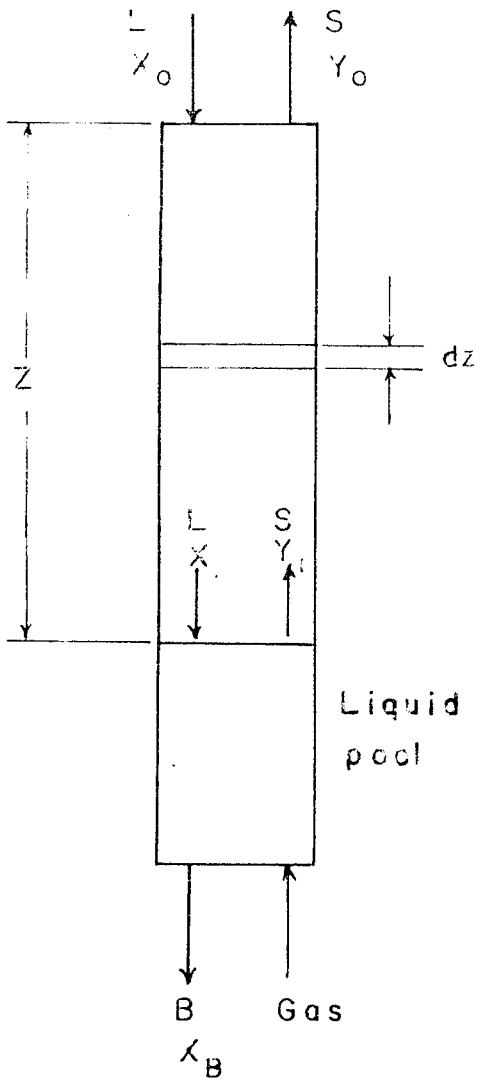

Figure 25. The counter-current foam column

This equation gives the value of y for any given value of x. It represents the operating curve and is a straight line for steady-state conditions.

The equilibrium curve given by Gibbs' equation is

$$y = x + \Gamma A$$

For EHDA-Br, Γ is constant. The equilibrium line is also a straight line if the area A per unit volume of foam is constant. The rate equations are

$$L\,dx = S\,dy = k_g\, a\, (y^* - y)\, s\, dz = k_L\, a\, (x - x^*)\, s\, ds \qquad (34)$$

where k_g = Mass transfer coefficient based on interfacial phase

k_L = Mass transfer coefficient based on liquid phase

a = Interfacial area per unit volume of foam

s = Cross-section of foam column

The foam column height may be calculated either in terms of interfacial phase compositions or in terms of bulk liquid phase compositions

$$Z = \frac{S}{k_g\, a\, s} \int_{y_1}^{y_o} \frac{dy}{y^* - y} \qquad (35)$$

$$Z = \frac{L}{k_L\, a\, s} \int_{x_1}^{x_o} \frac{dx}{x - x^*} \qquad (36)$$

The integrals in equations (35) and (36) are a measure of the difficulty of the operation. They are the usual "numbers of transfer units" and their coefficients which have units of length, are the HTU's. Thus height of foam column = HTU x NTU. The HTU can be determined experimentally using equation (35) or (36).

In the frequent case of linear operating and equilibrium line, the integral in equation (36) becomes

$$NTU_L = \int_{x_1}^{x_o} \frac{dx}{x - x^*} = \frac{x_o - x_1}{(x - x^*)_{lm}} = \frac{Z}{HTU} \qquad (37)$$

where

$$(x - x^*)_{lm} = \frac{(x_o - x_o^*) - (x_1 - x_1^*)}{\ln \frac{x_o - x_o^*}{x_1 - x_1^*}} \qquad (38)$$

In equation (37), only x_o can be measured directly. x_o^* is obtained from the equilibrium value corresponding to y_o, the concentration of the interfacial phase at the feed point, which can be approximated by the concentration of the collapsed foam if ample opportunity for drainage is provided by a drainage section above the feed point.

The liquid pool is assumed to be equivalent to one theoretical stage and the streams leaving this pool are in equilibrium. Therefore

$$y_1 = x_B + \Gamma A$$

A solute material balance around the liquid pool gives:

$$B x_B = L x_1 + S y_1$$

$$x_1 = \frac{B x_B - S y_1}{L}$$

x_1^* is the equilibrium concentration corresponding to y_1, i.e., x_B.

HTU values can be determined experimentally with the help of equation (37) and the information used for foam column design. This method has been used by Haas and Johnson (58) for foam columns separating Sr-89 and the HTU was found to depend on the type of feed distributor, gas sparger, on flow rates, etc.